CHALMERS
UNIVERSITY OF TECHNOLOGY

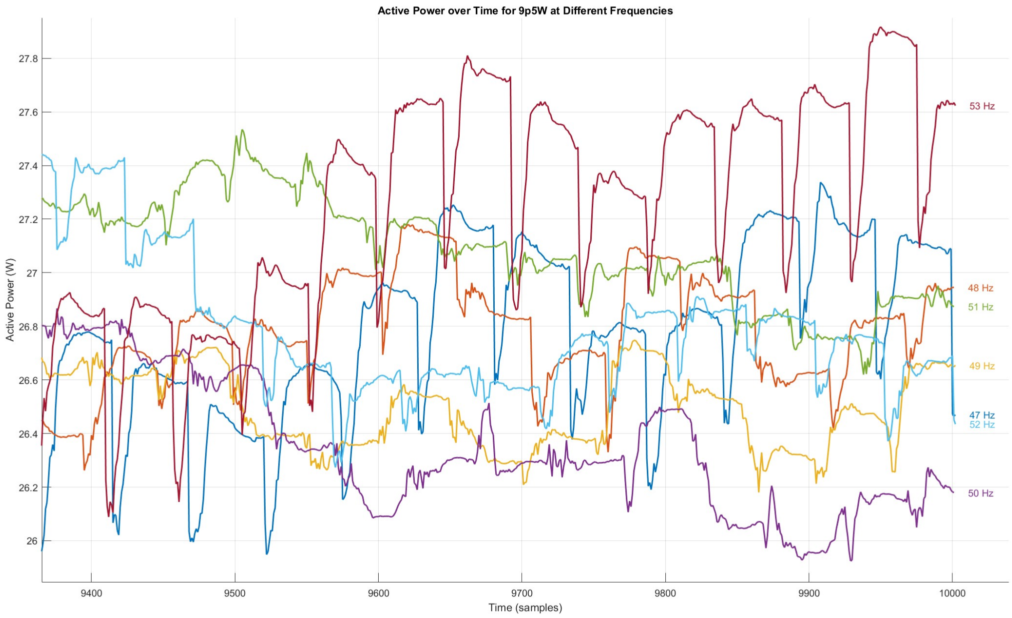

Frequency dependency of power system loads

Master Thesis

SUSTAINABLE ELECTRIC POWER ENGINEERING AND ELECTROMOBILITY, MPEPO

Almasbek Ayaz

DEPARTMENT OF ELECTRICAL ENGINEERING

CHALMERS UNIVERSITY OF TECHNOLOGY
Gothenburg, Sweden 2024
www.chalmers.se

Master's thesis 2024

Frequency dependency study of power system loads

A study of behaviour of different end-user loads under abnormal frequency conditions

ALMASBEK AYAZ

Department of Electrical Engineering
Chalmers University of Technology
Gothenburg, Sweden 2024

Frequency dependency study of power system loads
ALMASBEK AYAZ

Supervisor: Daniel Karlsson, DNV
Examiner: Peiyuan Chen, Department of Electrical Engineering

Master's Thesis 2024
Department of Electrical Engineering
Chalmers University of Technology
SE-412 96 Gothenburg

Typeset in LaTeX
Printed by Chalmers Reproservice
Gothenburg, Sweden 2024

Frequency dependency study of power system loads
ALMASBEK AYAZ Department of Electrical Engineering
Chalmers University of Technology

Abstract

The growing interest in examining power system loads is driven by the increasing integration of variable generation units into the distribution network. At the distribution level, load representation will involve smaller aggregates, such as smaller customer groups, resulting in aggregate load models and network performance being more sensitive to variations within the individual load components. As technological advancements in power systems emerge, it necessitates a more detailed representation of both the distribution network and the electrical characteristics of connected loads.

This study aims to understand the behaviour of these loads and investigate whether frequency dependency will become a critical parameter in future power system networks. Laboratory experiments were conducted to examine the frequency characteristics for both static and dynamic loads based on active and reactive power consumption. With the help of MATLAB analysing software, it was observed that static loads separately exhibited some frequency dependence; however, considering the combination of loads under evaluation, the frequency dependence coefficients are insignificant. This information enables a more thorough understanding of frequency dependence of loads.

Keywords: Power system, Load modelling, Frequency dependence, Load frequency characteristics, LED lightning, Induction machine, Electric heater.

Frekvensberoende studie av laster i elsystemet
ALMASBEK AYAZ Institutionen för elektroteknik
Chalmers Tekniska Högskola

Referat

Det växande intresset för att undersöka belastningar i kraftsystem drivs av den ökande integreringen av variabla produktionsenheter i distributionsnätet. På distributionsnivå innebär belastningsrepresentationen mindre aggregat, såsom mindre kundgrupper, vilket resulterar i att aggregerade belastningsmodeller och nätverksprestanda blir mer känsliga för variationer inom de enskilda belastningskomponenterna. När teknologiska framsteg inom kraftsystem uppstår krävs en mer detaljerad representation av både distributionsnätet och de elektriska egenskaperna hos anslutna belastningar.

Denna studie syftar till att förstå beteendet hos dessa belastningar och undersöka om frekvensberoende kommer att bli en kritisk parameter i framtida kraftsystemnätverk. Laboratorieexperiment genomfördes för att undersöka frekvensegenskaperna för både statiska och dynamiska belastningar baserat på aktiv och reaktiv effektförbrukning. Med hjälp av analysprogrammet MATLAB observerades att statiska belastningar separat uppvisade viss frekvensberoende; dock, när man betraktar kombinationen av belastningar, är frekvensberoendekoefficienterna obetydliga. Denna information möjliggör en mer grundlig förståelse av belastningars frekvensberoende.

Nyckelord: Kraftsystem, Lastmodellering, Frekvensberoende, Lastfrekvensegenskaper, LED-belysning, Induktionsmaskin, Elektrisk värmare.

Acknowledgements

Firstly, I would like to express my gratitude to my supervisor, Daniel Karlsson, for his honesty, patience, and continued support throughout the Master Thesis. I also extend my thanks to the thesis examiner, Peiyuan Chen, for his time and effort in reviewing the thesis. Reaching this milestone would not have been possible without the support of my friends and family during my studies. I am deeply thankful for their encouragement; without their belief in me, achieving success would have been much more challenging.

Almasbek Ayaz, Gothenburg, June 2024

List of Acronyms

Below is the list of acronyms that have been used throughout this thesis listed in alphabetical order:

AC	Alternating current
CDF	Cumulative Distribution Function
CIG	Converter-Interfaced Generation
CIGRE	International Council on Large Electrical Systems
DC	Direct current
DER	Distributed Energy Resource
DESS	Distributed Energy Storage System
EV	Electric Vehicle
IEEE	Institute of Electric and Electronic Engineering
IM	Induction Machine
MG	Microgrid
PV	Photovoltaic
RES	Renewable-based Energy Sources
RMS	Root Mean Square
SPIM	Single-phase Induction Machine
WECC	Western Electricity Coordinating Council
ZIP	Polynomial Load Model
3PIM	3-phase Induction Machine

Nomenclature

Variables

P	Active power
Q	Reactive power
U	Voltage
f	Frequency
θ	Displacement angle
k_{pu}	Exponential load model parameter (active power)
k_{qu}	Exponential load model parameter (reactive power)
k_{pf}	Load frequency sensitivity parameter (active power)
k_{qf}	Load frequency sensitivity parameter (reactive power)

Contents

List of Figures

List of Tables

1

Introduction

1.1 Background

Power system simulation is essential for planning and operating a power systems. The growing interest in studying power system loads is driven by the increasing integration of variable generation units into the distribution network, which will cause significant effect on end-user loads. Thus it necessitates a more detailed representation of both the distribution network and the connected loads. Simulation outcomes heavily rely on accurate models of system components, such as generators, excitation systems, transformers, lines, loads, and other related equipment. Among these, system loads are particularly challenging to model due to their diversity and complexity. Understanding loads is crucial, especially when power systems are operated near their stability limits. Loads encompass various devices in a power system that consume electrical energy, including motors, lamps, office equipment, home appliances, and more.

This thesis work is aimed to gain knowledge on how load power consumption varies with the frequency variations. For the frequency variation studies "bottom-up" or component-based method is used. This method suggests to gain extensive knowledge on end-use electrical load data and use it to do the power system simulations. Based on data from Swedish Energy Agency, electricity appliances are distributed among lighting, home electronics, refrigerator and cooking equipment. Available equipment in the laboratory makes it possible to simulate the behaviour of the end-use electrical loads. Using the full digital, full 4 quadrant 3-phase AC power sources Regatron TC.ACS and synchronous generator, abnormal frequency variations were simulated and parameters were measured. Then all obtained data was analyzed using MATLAB and the results are analyzed and discussed in this thesis.

1.2 Objectives

The main objective of this thesis is to understand how the load objects react to frequency variations under abnormal operational conditions. It is crucial to mitigate the most serious consequences of disturbances and power imbalances. Applying modelling approaches this study will be focused on frequency dependence of loads in laboratory environment and observation of the active and reactive power consumption for static and dynamic loads. The first step for this study is to do a literature review on different load types and review of observed frequency dependence. Then, using the approaches indicated in this work residential load types will be listed and tested for frequency dependence.

1.2.1 Research questions

For the studies considered in this thesis next research questions applied.

1. How the load components have changed in last years?
2. How the load components behave under different frequency variations?
3. How the load frequency dependence changes in last years?

Review of previous studies was conducted to develop representative load models. Additionally, frequency measurements were performed in a laboratory environment, and the behavior of these load models was analyzed based on the obtained data.

1.3 Literature review

Decisions in electrical power systems planning and operation rely heavily on the outcomes of power flow and stability simulation studies. Achieving realistic results necessitates precise modelling of all network components, underscoring the importance of accurately representing loads and their electrical characteristics. This is particularly critical in distribution systems, where aggregate loads are smaller, and each type of load can significantly impact power system operations. Furthermore, changes in technological trends or the implementation of performance legislation are likely to modify the electrical characteristics of loads. This section discusses previous studies regarding load frequency characteristics of different types of loads and the methods of load modelling.

With the increasing penetration of renewable energy sources(RES), significant challenges will arise concerning the normal operation, control, and planning of power systems to maintain current levels of supply security. Beyond supplying energy to end-users, power system operators' primary responsibility is to ensure the reliability and security of the supply. A crucial aspect of this security is the load-generation balance. Any imbalance between the active power generated and the electrical load causes frequency deviations, which can degrade the power system's performance. Thus, frequency serves as a valuable indicator of the balance between generation and load.[1] [2]

Technological advancements and new performance legislation are likely to modify the electrical characteristics of loads. Since the last comprehensive review of load modeling, current load models exhibit several differences from previously developed models of similar load types. This underscores the necessity of continually updating load models to reflect these changes.[3]

1.3.1 Literature review on Load modelling

Loads function as dynamic systems. With the involvement of Converter-Interfaced Generations (CIGs), storage devices, and load-side controllers, the dynamics of aggregate loads will become more complex and may exhibit rapid changes. According to [4] CIGs will play an increasingly significant role in frequency control, underscoring the importance of developing accurate load models.

It was stated in [5] the introduction of new devices (e.g., smart devices), new vehicles (e.g., electric cars), advanced building technologies, and new building standards (e.g., passive or zero-energy houses) will influence the residential electricity load profile. According to the author Proedrou et. al. [5] new load models will pose challenges for both short-term and long-term forecasting. Investigating the effects of these new appliances on residential electricity load models represents a significant research direction. This research facilitates the analysis of the impact of smart homes on future residential load profiles, thereby aiding in the development of effective plans and strategies.

Including load characteristics in dynamic calculations is essential for achieving more accurate results and minimizing frequency deviations. Experimental measurements in [6] confirm that home appliances exhibit different behaviors at varying frequencies, resulting in distinct static frequency characteristics for each appliance. These findings are subsequently utilized to develop a simplified model of frequency control, highlighting their significant impact on the accuracy and reliability of dynamic calculations.

1.3.2 Literature review on load types

With the advancement of smart electric transportation systems, the large-scale deployment of electric vehicles (EVs) is anticipated in the near future. If EVs participate in frequency regulation, their charging power will fluctuate, resulting in variable power losses attributed to EVs. The study in [7] concentrated on modeling power losses due to EVs and constant current loads in the network. When approaching the line limit in the aggregate EV model, transformers and distribution lines may become overloaded.

Both residential and industrial consumers rapidly transitioned to LED technology due to its economic and environmental benefits. LED lamps necessitate a power processing unit, typically a power electronics driver, which is inherently non-linear. In the study by H. Shabbir et al.[8], LED lamps are classified into three categories: Good, Average, and Poor. When good LEDs were replaced with poor LEDs, both the constant current injection method and the iterative harmonic analysis demonstrated significant increases in distortion and harmonic losses. However, the results from the iterative harmonic analysis differed from those of the constant current injection method. This discrepancy is attributed to the iterative harmonic analysis accounting for the voltage-dependent current behavior of LED lamps and the attenuation effect. Therefore, there is a need for the future research on LED lamps' quality, behavior and harmonic pollution in power systems.

A study represented in [9] indicates the influence of supplied power on heating transient. It states that the distributions of current density and specific power in a ferromagnetic workpiece (heating element) are influenced by the size and shape of the cross-section, the intensity of the current flow, and the temperature. However, the current flowing through the workpiece is a complex function of the voltage (U), external reactance (X_ext), and the impedance (Z_w) of the workpiece, which itself varies with current and temperature values. The study presents data indicating that, at a constant voltage, an increase in the X_{ext} leads to a reduction in the maximum current (I_m), the maximum active power (P_m) delivered to the workpiece, and a decrease in the average power factor ($\cos \phi_m$) of the installation.

Numerous studies on the utilization of demand-side resources for frequency regulation have primarily focused on customer-side batteries, electric vehicles, and thermostatically controlled loads (TCLs), including water heaters, heating, ventilation, and air-conditioning (HVAC) units, and refrigerators. [10] propose a straightforward data-driven methodology for providing frequency regulation using residential HVAC units. This proposed methodology employs an aggregated residential load model, which is derived from low-resolution load data.

1.3.3 Literature review on Load modelling methodologies

The component approach, also referred to as the knowledge-based approach, is a modeling methodology that operates from the ground up. It involves deriving an aggregated load model by considering: 1) Identifying load classes connected to a substation, 2) Understanding the structure and composition of load categories or components within each load class, and 3) Examining typical characteristics of each load category or component. This aggregated model integrates key individual load components and is often represented as a second-order polynomial model coupled with an induction motor model or as a composite load model. This approach to load modeling establishes a standardized load model structure along with a corresponding set of parameter values that are consistently applied throughout the system model [11].

The measurement-based approach adjusts the most sensitive parameters of the load model to align with an event by utilizing optimization algorithms that minimize the discrepancy between the model and actual data measurements. This methodology typically yields the most precise representation of the model's response to real events. However, the parameters derived through this approach often lack generalizability, necessitating the repetition of the process for each individual event. [12]

Authors in [13] states that comprehensive information regarding the load mixture is not consistently accessible, and in that paper an alternative approach involving measurement-based methods has been suggested. This method entails utilizing data obtained from field measurements or detailed dynamic simulations.

The findings in [14] underscore the necessity of employing measurement-based methods, alongside potentially other time-series data curve fitting techniques within power systems, to assess the assumption that system response error correlates with system accuracy. It is unwise to presume that measurement-based approaches utilizing similarity measures automatically yield insightful outcomes. Any optimization or estimation technique predicated on minimizing system response error will produce inaccurate findings without a robust correlation between system response error and system accuracy.

Due to the complexities associated with measurement-based parameter estimation, a component-based approach is more pragmatic for extensive studies in dynamic load modeling. Nevertheless, in the absence of detailed information on the distribution of consumer classes (i.e., the proportion of each consumer type aggregated at a given substation), accurately assessing the impact of each consumer on the grid becomes challenging. [12]

1.3.4 Literature review on studies of the behavior of different loads in power systems

In [14] variations in control parameters, such as frequency and voltage variations within motor models were tested. A potential discrepancies in methodology of observation across such models can induce oscillations at varying frequencies. It is crucial to accurately capture specific output alterations, as they hold significant reliability implications for utility operations. Delays in the frequency containment or restoration to the standard 60 Hz frequency in the United States can lead to regulatory penalties. It was stated in the study that experiments of load model accuracy in system level and in bus level show lack of error-response correlation

Study in [15] presents the synergetic control aims to swiftly utilize available flexible load resources to enhance system stability during low-demand periods, thereby achieving improvements in system performance. However, it also aims to prevent excessive responsiveness that could lead to frequency overshoot. Applied component based approach investigates resistive loads as fridge, freezer along with water and space heaters. The paper includes study about charging load and its behavior in power system.

In [13] the aim of the paper is to explore how various static load models affect studies related to small-signal, transient, and frequency stability. Specifically, the paper examines the exponential and polynomial load models, considering implementations that account for voltage and frequency dependencies. Multiple parameter sets are evaluated to assess their influence on the outcomes of system stability studies.

I. D. Pasiopoulou et al.[13] delves deeper into the influence of the frequency-dependent factor on bus voltages, examines the Key Performance Indicator (KPI) through cumulative distribution functions (CDFs). As depicted, both load modeling and the location of the disturbance impact the maximum Rate of Change of Frequency (RoCoF) value. To gain insight into all system buses, we conduct a statistical analysis of the maximum RoCoF using Cumulative Distribution Functions (CDFs).

The research of [6] focused on investigating the response of household appliances to variations in the frequency of the supplied voltage. Frequency characteristics were measured within the 46.9 to 53.1 Hz range, which was selected to cover both on-grid and off-grid network operations. In order to comprehensively assess appliance behavior, measurements were conducted from the lowest to the highest frequency, and vice versa, forming a complete loop across the frequency range. A frequency step of 0.01 Hz was utilized, with a constant voltage setting of 230 V maintained throughout all measurements.

2

Theory on power system loads

In this section theoretical knowledge about the load model types, load components and the universal standard for measurement is represented.

2.1 Load models

In power system analysis, both steady-state and dynamic load modeling are crucial for understanding system behavior and ensuring stability. The most commonly utilized load models, regardless of the methodology employed in their development, can be systematically categorized into two primary groups: static and dynamic.

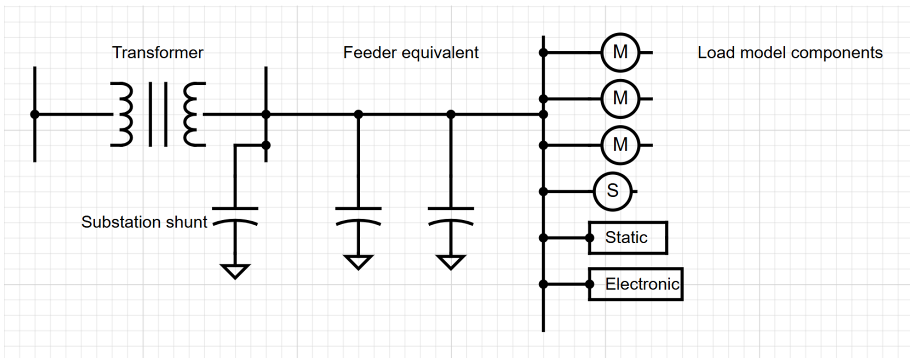

Figure 2.1: WECC Composite Load Model

2.1.1 Static Load Models:

Static load models encompass exponential, polynomial, linear, comprehensive, static induction motor, and power electronic-interfaced models. These load models depict the correlation between active and reactive power consumed by a specific load as an algebraic function of voltage and frequency. When modeling the dynamic characteristics of the load, its dynamic model can be developed separately from its static load model. Alternatively, if the dynamic load model is already established, deriving the static load model from the existing dynamic load model is a straightforward process.[11]

2.1.1.1 Static load model types

1. Constant Power Load (CPL): CPL models assume that the load consumes a constant amount of real power irrespective of voltage variations. It's commonly used to represent loads such as electronic equipment and lighting.

2. Constant Current Load (CCL): CCL models represent loads that draw constant current regardless of voltage variations. This model is often applied to represent arc furnaces and welding equipment.

3. Constant Impedance Load (CIL): CIL models assume that the load behaves as a constant impedance, meaning the load consumes a constant ratio of voltage to current. This model is suitable for representing loads like heating elements and electric motors.

4. ZIP Load Model: The ZIP model divides the load into three components: constant impedance, constant current, and constant power. This model provides a more detailed representation of load behavior compared to individual constant load models.

$$P = Pn(\frac{U}{Un})^{k_{pu}}(\frac{f}{fn})^{k_{pf}}. \tag{2.1}$$

$$Q = Qn(\frac{U}{Un})^{k_{qu}}(\frac{f}{fn})^{k_{qf}}. \tag{2.2}$$

2.1.2 Dynamic Load Models:

Dynamic load models comprise exponential dynamic load models, dynamic induction motor (IM) models, transfer function IM models, composite models, distribution models, bulk power bus load models, and distributed energy storage system (DESS) models. Dynamic loads exhibit time-dependent responses that are influenced by the preceding states or conditions of both the system and the load itself. The dynamic response is also affected by the interactions and energy exchanges between the system and the load during and after the transition from one state or condition to the next. It is important to note that both static and dynamic load models can be employed in dynamic studies.[11]

In contrast to static load models, dynamic load models offer analytical frameworks to elucidate the behavior of real and reactive power loads within a prescribed voltage and system frequency setting, typically expressed through differential equations. Dynamic load models commonly encapsulate the characteristics of loads characterized by successive power fluctuations in response to alterations in voltage or system frequency across various buses within the network.(IEEE Guide for Load Modeling and Simulations for Power Systems) The analysis further revealed that static load models remain predominant, even in investigations of dynamic systems. Moreover, it indicated that merely about 30% of utility companies and transmission system operators incorporate dynamic load representation through various iterations of the IM model. [11]

2.1.2.1 Dynamic load model types

1. Dynamic Exponential Load Model: The exponential load model represents the dynamic response of loads by using a first-order differential equation. It captures the gradual change in load following a disturbance and is often used for modeling induction motors and other electromechanical loads.

2. Composite Load Model: The composite load model combines static and dynamic elements to represent a more realistic load behavior. It includes components such as constant power, constant current, and dynamic response characteristics, allowing for a more accurate representation of load dynamics during transient events.

3. Motor Starting Models: Motor starting models simulate the dynamic response of induction motors during startup. These models consider factors such as motor inertia, acceleration, and torque characteristics to accurately predict the impact of motor starting on system stability.

4. Frequency-Dependent Load Models: These models incorporate frequency - dependent behavior into load representation, which is particularly important for analyzing the impact of frequency deviations on load dynamics. They capture phenomena such as load shedding and frequency-dependent load response.

5. Load Shedding Models: Load shedding models simulate the controlled disconnection of loads during system emergencies to maintain stability. These models are essential for assessing the effectiveness of load shedding schemes and optimizing their implementation.

These are just a few examples of the load models commonly used in both steady-state and dynamic power system analysis. The choice of load model depends on factors such as the level of detail required, the type of load being represented, and the specific objectives of the analysis.

2.2 IEEE Standards for Measurement of Electric Power Quantities

The current definitions for active, reactive, and apparent powers are rooted in the understanding established and accepted during the 1940s. These definitions were effective for the industry as long as the current and voltage waveforms remained nearly sinusoidal.[16]

This standard aims to extend well-established concepts by providing updated definitions. It is intended for users involved in measuring and designing instrumentation for energy and power quantification. It is not designed to assist in the real-time control of dynamic compensators or for diagnostic instrumentation used to identify specific types of disturbances or harmonics.

Accpording to the standards power consumptions are calculated[16].

1. Single phase sinusoidal Active power calculation

   The active power P, also known as real power, is the average of the instantaneous power over the measurement period from τ to $\tau + kT$.

   $$|P = \frac{1}{kT}\int_{\tau}^{\tau+kT} p\,dt = \frac{1}{kT}\int_{\tau}^{\tau+kT} vi\,dt \tag{2.3}$$

   where, $T = \frac{1}{kT}$ is the cycle time (s), k is a positive integer number, τ is the moment when the measurement starts, the component pa is the instantaneous active power.

2. Single phase sinusoidal Reactive power calculation

   $$|Q = \frac{w}{kT}\int_{\tau}^{\tau+kT} i[\int vdt]\,dt \tag{2.4}$$

   If the load is inductive, then $Q > 0$. If the load is capacitive, then $Q < 0$. This means that when the current lags the voltage $\Theta > 0$ and vice versa.

3. Fundamental of Active and Reactive power

   The fundamental of active and reactive power is commonly associated with the fundamental frequency. In a 50 Hz power system, P_1 is often referred to as "50 Hz active power."

2.3 Ligth Emitting Diodes (LEDs)

Around the globe, emerging companies specializing exclusively in LED technologies are emerging, posing challenges to conventional lighting companies. This trend is accelerating the market shift towards significant reductions in CO2 emissions. Market participants are rapidly innovating, with firms creating and launching progressively efficient products boasting superior performance, smart functionalities, and high-quality lighting.[17][18]

LED technology stands out as the most efficient means of converting electrons into photons. Additionally, it presents advantages such as extended lifespan, seamless integration with lighting controls, enhanced optical control, improved dimming capabilities, and color versatility. From the standpoint of a circular economy, LED light sources exhibit minimal environmental impact, making them the optimal choice when considering the entire product life cycle.

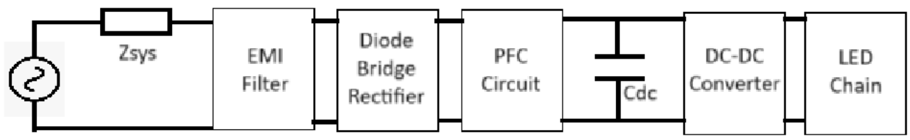

Figure 2.2: High-power LED schematic

LED lighting has already demonstrated significant cost-effectiveness when contrasted with traditional lighting sources, particularly incandescent, halogen, and fluorescent lamps. Industry advancements have led to the development of direct, plug-and-play LED products, eliminating the need for fixture replacement. These retrofit LED solutions enable existing fixtures to be retained while end users reap the advantages of notably reduced operational expenses. In comparison to incandescent lamps, LED bulbs deliver energy savings ranging from 80% to 90%. When compared to fluorescent lamps, LED lighting achieves savings ranging from 50% to 60%.[19]

LED drivers are generally categorized into AC and DC types. AC LED drivers are typically straightforward and passive in design. While simple AC-driven LED systems benefit from low cost and circuit simplicity, they often exhibit inefficient utilization of LED lamps. In contrast, there has been a recent trend towards the use of DC drivers in LED lamps. DC LED drivers can deliver a more continuous luminous output due to the steady DC component. Most DC LED drivers are based on established switched-mode power supply techniques and topologies, such as buck, SEPIC, Cuk, and boost converters.[20]

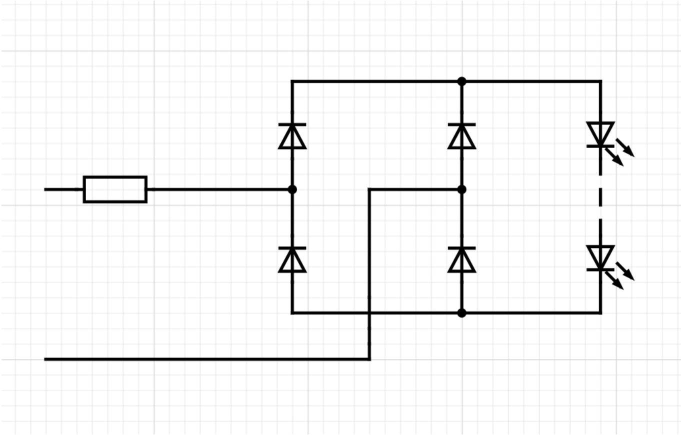

Figure 2.3: Simple passive driver using DC rectification[20]

In [20] input capacitor was incorporated across the input AC voltage to correct the input power factor of these overall inductive circuits to unity. The core losses in the input and output inductors have been identified as the primary sources of power loss. Losses in the input inductor are influenced by input current harmonics, whereas the core losses in the output inductor are attributed to the output current ripple, which is, in turn, caused by the output voltage ripple.

Also as stated in [8] a crucial aspect in the design of an LED driver is the minimization of capacitance and inductance, while still adhering to the necessary electrical performance criteria, such as minimizing the levels of output voltage and current ripple.

One prominent trend in the lamps and lighting sector is the widespread embrace of LED technology. LED lighting solutions are renowned for their exceptional energy efficiency, extended durability, and diverse array of color temperatures and lighting effects. Consequently, LED lighting solutions have emerged as the preferred option for consumers.

Another notable trend in this domain is the surging interest in smart lighting solutions. These smart lighting solutions enable remote control via smartphones or voice assistants, offering a host of functionalities including color adjustment, dimming, and scheduling. With the rising adoption of smart home technologies, smart lighting solutions are gaining traction among consumers. [21]

2.4 Motors

The load model structures employ an "equivalent" induction machine to depict the dynamic attributes of loads. The extent of detail in modeling the induction motor varies based on the specific study requirements. For load modeling purposes, a third-order model suffices, encompassing rotor flux and speed dynamics. Precisely, the machine is represented using three states: rotor d-axis and q-axis fluxes, along with rotor speed. The model disregards stator dynamics.

The final distinction among motor types pertains to the mechanical load applied to the rotor shaft. These loads are typically categorized into three main types: variable torque (VT), constant torque (CT), and constant mechanical power (CP) loads. Variable torques can further be classified into quadratic (QT) and linear torque (LT) based on whether the torque is directly proportional to the motor speed or to the square of the motor speed, respectively. Examples of variable torque loads include centrifugal pumps and fans. Constant torque loads comprise compressors, conveyors, and traction drives. In the case of constant mechanical power loads, the torque varies inversely with the motor speed, with examples including grinders and winders.[22]

2.4.1 Induction machine

Due to their large numbers, IMs are typically represented by a distinct load model. Another reason for this separation is that IMs significantly impact the dynamic characteristics of the aggregate load. The complex dynamic behavior of IM loads is usually captured in power system analysis using the 'dq' reference frame transformation. This transformation converts the three-phase AC quantities into a system of equations based on only two axes. The standard 'dq' representation of a symmetrical three-phase induction motor is provided by equations below.[18]

1. Stator flux linkage

$$\Psi_{sq} = L_s \times i_{sq} + L_m \times i_{rq} \tag{2.5}$$

$$\Psi_{sd} = L_s \times i_{sd} + L_m \times i_{rd} \tag{2.6}$$

2. Rotor flux linkage

$$\Psi_{rq} = L_r \times i_{rq} + L_m \times i_{rq} \tag{2.7}$$

$$\Psi_{rd} = L_r \times i_{rd} + L_m \times i_{sd} \tag{2.8}$$

3. Stator voltage

$$v_{sq} = R_s \times i_{sq} + \frac{d}{dt}(\Psi_{sq}) + \omega_s \times \Psi_{sd} \tag{2.9}$$

$$v_{sd} = R_s \times i_{sd} + \frac{d}{dt}(\Psi_{sd}) - \omega_s \times \Psi_{sq} \tag{2.10}$$

4. Rotor voltage

$$v_{rq} = R_r \times i_{rq} + \frac{d}{dt}(\Psi'_{rq}) + (\omega_s - \omega) \times \Psi_{rd} \tag{2.11}$$

$$v_{rd} = R_r \times i_{rd} + \frac{d}{dt}(\Psi'_{rd}) - (\omega_s - \omega) \times \Psi_{rq} \tag{2.12}$$

5. Mechanical equation

$$J\frac{d}{dt}(\omega) = Te - Tm \tag{2.13}$$

6. Torque equation

$$T_e = \frac{3n_p}{2}\times(\Psi_{sd}\times i_{sq} - \Psi_{sq}\times i_{sd}) \tag{2.14}$$

7. Power equations

$$T_e = \frac{Pe}{\Omega_r} = \frac{n_p P_e}{\omega_r} \tag{2.15}$$

$$P_e = \frac{3n_p}{2}\times(\Psi_{sd}\times i_{sq} - \Psi_{sq}\times i_{sd}) \tag{2.16}$$

Induction motors IMs with direct connection find applications in various fields such as refrigerator/freezers, washing machines, and dishwashers. Within the residential load sector, the prevalent usage consists of single-phase IMs (SPIMs), which are also commonly employed in commercial settings. Larger facilities in the commercial sector may opt for three-phase IMs (3PIM), provided that such connections are available. Due to thorough representation in existing literature, the electrical models pertaining to this load category are not extensively examined in this thesis.

2.5 Electric heating

Radiators and furnaces are typically modeled as constant impedance loads, while heat pumps are modeled as induction motors. The fundamental operating principle of electrical space and water heating loads involves a resistive heating element that heats the surrounding air or water.

As it was said in [9] resistance heating can be applied in two ways: direct resistance heating, where the material to be heated itself carries the current and generates heat internally, and indirect resistance heating, where heat is produced in a separate conductor or heating element. For effective heating through direct resistance, a significant portion of the total available power must be dissipated within the workpiece. The workpiece resistance must be relatively high compared to the supply circuit. It should match the supply to ensure maximum current at the rated voltage.[9]

1. Direct Resistance Heating (DHR) Power calculation

$$P'_{tot} = (R_{tr} + R_{hc} + R_c + R_w){I_2}^2 + P_o \tag{2.17}$$

$$P_a = U_2\times I_2 \tag{2.18}$$

$$cos(\phi) = \frac{P_{tot}}{P_a} \tag{2.19}$$

According to the [23], electricity remains the most prevalent source of energy for space and water heating in homes. One-third of households rely solely on electricity for heating, with half of these using direct-acting electricity, which includes both resistive heaters and the electrical energy consumed by heat pumps.

2.6 Load Frequency Characteristics

The analyzed outputs of the measurements include the values of active power P and reactive power Q for each measured frequency and timestamp. From this data, the frequency bias factor(K) and the frequency sensitivity coefficient (K_{xf}) for all measured quantities were calculated as follows:

$$\text{frequency bias factor} \quad K = \frac{\Delta P}{\Delta f} \quad [\text{W/Hz}] \tag{2.20}$$

$$\text{frequency sensitivity coefficient} \quad K_{Pf} = \frac{\Delta P}{\Delta f} \times \frac{1}{P_n} \quad [1/\text{Hz}] \tag{2.21}$$

$$\text{frequency sensitivity coefficient} \quad K_{Qf} = \frac{\Delta Q}{\Delta f} \times \frac{1}{Q_n} \quad [1/\text{Hz}] \tag{2.22}$$

Table 2.1: Typical kp, kq values for different loads[24]

Component	*Powerfactor*	k_{pf} [1/Hz]	k_{qf} [1/Hz]
Refrigerator	0.80	0.41	-0.94
Incandescent lights	1.00	-0.01	-0.99
LED lamps	0.90	0.00	0.51
Electrical motors	0.88	2.50	1.20
Motor drives as Hair dryer	0.87	0.18	1.35
Water pumps	0.85	5.00	4.00
Arc furnace	0.70	-1.00	-1.00
Transformer	0.64	0.00	-11.8

3
Parameter determination methods

After determining the type of load model, the next step involves identifying the parameter values associated with the model. It's important to acknowledge that, in certain instances, determining the structure of the load model may depend on understanding the electrical characteristics of the load beforehand. Two commonly utilized methods for determining parameter values are the measurement-based approach and the component-based approach. While the discussion below pertains to the development of aggregate load models, the fundamental principles can also be applied to formulate individual load models.[11]

3.1 Component-based approach

The component-based load modeling approach is often characterized as a "bottom-up" approach because it involves constructing the aggregate load model from the individual load components within it. One key advantage of this approach is that it does not require measurements of the power system to develop the aggregate load model. However, to compensate for this, extensive data collection is necessary to determine the load composition of the modeled aggregated load.[18]

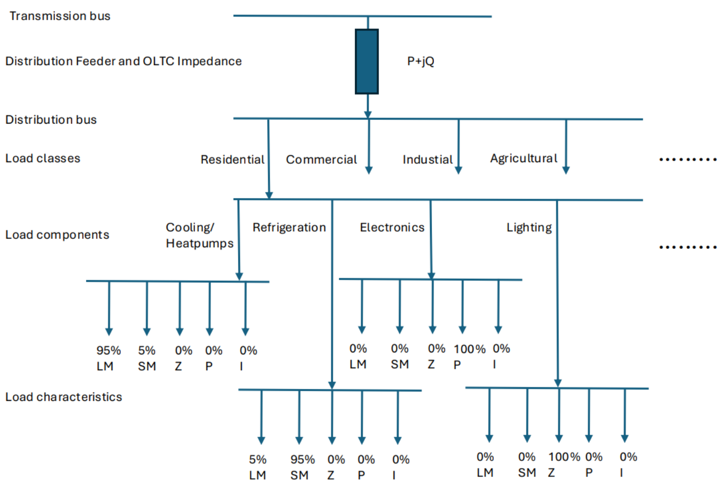

Figure 3.1: Example of Component Based Approach[11]

Based on Figure 3.1, the total load supplied at a bus can be classified into load classes according to their consumption patterns, generally categorized as residential, commercial, and industrial at the highest level. Conversely, it is advised to model large industrial loads with as much precision as feasible, utilizing data tailored to the respective plants. Representing typical load classes poses greater challenges due to the dispersed nature of the load and the potentially extensive data prerequisites.[18]

Once load classes are identified, the subsequent stage involves determining load components and their respective proportionate contributions within each class. These load classes encompass typical components, such as lighting, air conditioning, space heating, water heating, and refrigeration, which collectively constitute the majority of power consumption by end users. The difficulty lies in ascertaining the percentage contributions of each load component within the designated load class. Acquiring this data, which varies across networks and geographic locations and evolves over time, typically entails a time-consuming and intricate process, often reliant on customer surveys.

Table 3.1: Electricity use in the industrial sector, by industry for 2020, Sweden[23]

Name	*Electricity consumption*(TWh)
Pulp and paper	18.9
Steel and metal	7
Chemical	5.1
Mechanical engineering	4.7
Mining	3.9
Food, beverages, tobacco	2.4
Non-metallic minerals	0.9
Wood products	1.7
Small industries and other	2.2

3.2 Measurement-based approach

The measurement-based approach, also known as the "top-down" methodology, utilizes system events and disturbances observed at representative substations and feeders to deduce the characteristics of the connected load. This approach is alternatively termed a "behavior-based" method, as it involves recording both static and dynamic responses of the loads, which are then employed to formulate the necessary load model. To develop load models and estimate reliable parameters, it is crucial to establish the initial load model structure beforehand. Illustratively, the measurement-based approach is depicted in Figure 3.2, where circles denote current transformers monitored at the feeder head or on the low voltage side of step-down transformers, and square symbols represent voltage transformer measurements. The associated recording equipment captures the load response to all events occurring upstream at the higher voltage level. During system disturbances, the load response is measured by the recorders, but the load can also be monitored and recorded during normal operation.[14]

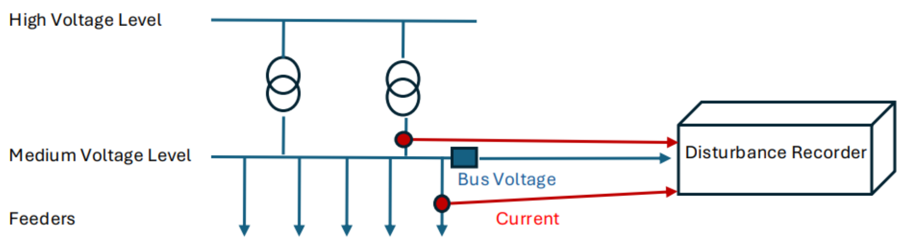

Figure 3.2: Example of Measurement Based Approach

The parameters of the load model are determined by fitting measured data to the presumed model structure, employing parameter identification and curve fitting techniques. More intricate models may necessitate the use of complex estimation techniques, particularly depending on the types and quantity of disturbances present in the recorded data sets. The identification process involves selecting a suitable performance function and determining load model parameters to accurately replicate the loads' dynamic response during and after a disturbance. This is achieved by analyzing the correlation between alterations in voltage and/or frequency and the corresponding fluctuations in load active and reactive power demand.[14]

Power system simulation is crucial for planning and operation, especially with the increasing integration of variable generation units in the distribution network. Accurate simulation relies on detailed models of system components, including generators, excitation systems, transformers, transmission lines, and loads. Among these, system load modeling is particularly challenging due to its diversity and complexity. Understanding load behavior is essential, especially when power systems operate near their stability limits. Load includes various electrical energy-consuming devices such as motors, lighting, office equipment, and household appliances.[18]

There are advantages and disadvantages of these two methods. Those aspects of methods are mentioned in the Table 3.2.

Table 3.2: Pros and cons of methods

Component-based	Measurement-based
+ Does not require field measurements.	+ Does not necessitate extensive knowledge or information gathering on load component.
+ Provides knowledge about the load types.	+ Can be applied to any load.
+ Can be applied in any location with a similar load class mix.	+ Suitable for estimating load parameters at bulk load buses.
- Complexity in gathering information. It can be difficult to find representative parameter values.	- Less reliable at lower voltage levels.
- The same load component can have different predefined parameter values, requiring the selection of the most appropriate one.	- The load response is constrained by the magnitude of the disturbance.
- Categorizing new types of loads based on predefined load components can be challenging.	- This method may yield spontaneous solutions or no feasible solution at all in optimization algorithms.

4
Laboratory experiments

The aim of this thesis research is to offer an adaptable approach to load modeling that can effectively analyze contemporary and forthcoming power systems. To achieve this, it's essential to choose the most versatile load modeling techniques and ensure that the developed load models are adaptable for use across various power system analyses. This objective is optimally realized by component-based load modeling framework.

The exponential and polynomial load model forms are chosen to depict the load behaviors during steady-state power flow analysis and some dynamic studies. Consequently, the results are presented in the most applicable format. These models are derived by altering the frequency within the range of f = [47, 53 Hz], and the total active and reactive power requirements for each frequency are computed based on the input current and voltage waveforms. As these models aim solely to convey data regarding the active and reactive power magnitudes, they do not include any details about the harmonic emissions of modern power system loads.

Figure 4.1: Regatron TC.ACS

A full digital, full 4 quadrant 3-phase AC power sources Regatron TC.ACS and synchronous generator were used to vary the frequency parameters. For the Regatron TC.ACS in order to measure the current, voltage and frequency waveforms Microlab digital meter was used. With obtained waveforms using the MATLAB and accoerding to IEEE 1459-2010 standard power waveforms were computed. During the study power consumptions at steady-state frequencies were studied. Most of the loads were single-phase loads and connected to the power supply between one phase and neutral.

4.1 Laboratory setup

4.1.1 LED lamp setup

For the frequency dependency studies of lighting loads several types of LED lamps from different manufacturers were used. With the help of Regatron TC.ACS, it was possible to study LED lamp behavior for different steady state frequencies. The main focus of this research is to observe active and reactive power consumption of the lamps. Simple LED lamps schematic is presented to give broad information about the testing process.

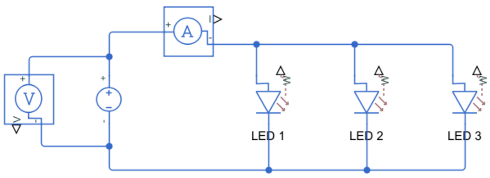

(a) LED schematic

(b) LED setup

Figure 4.2: Lamp setup for laboratory test

Three LED lamps of the same wattage were connected in parallel using simple laboratory setup. In order to choose the lamps used in residential sector convenient stores were asked about the popular lamps. Unfortunately, they did not provide a document because of the confidential information.

4.1.2 Heater setup

The electric heater used for this study is the resistor accompanied by the fan. As it was mentioned in literature review it can be classified as the direct resistance heating with the heating element. The purpose of this tests was to investigate the influence of frequency on active and reactive power consumption of the heating fan.

Figure 4.3: Heater setup

4.1.3 Induction Machine setup

For an induction machine frequency dependency test synchronous generator and IM with different loading conditions were used. Different loading conditions represent different types of IMs in use. For this test 3 loading conditions were applied: 0kW, 7.5kW and 15kW load. Using the dSPACE Control Desk software actual active and reactive power values were recorded.

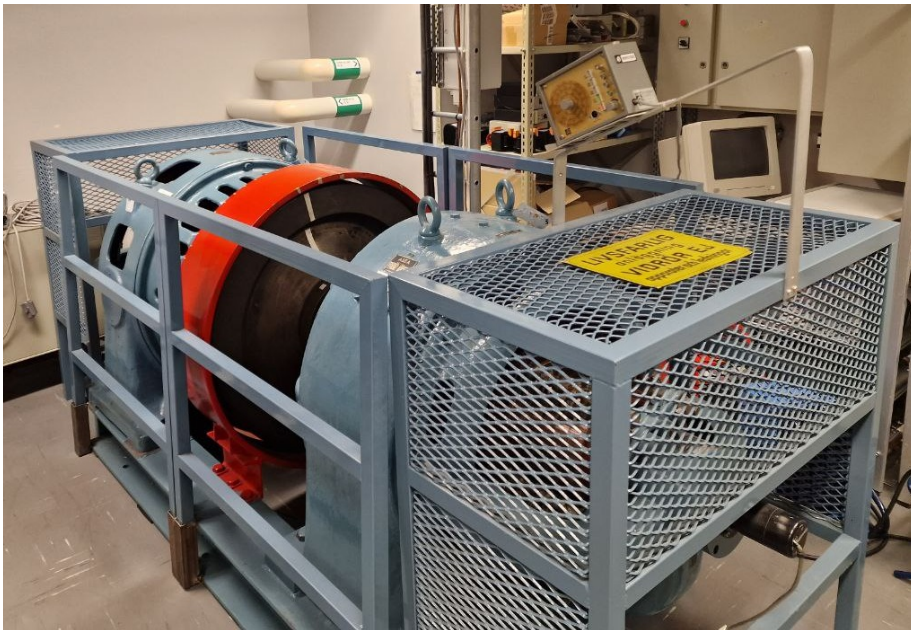

Figure 4.4: Synchronous machine

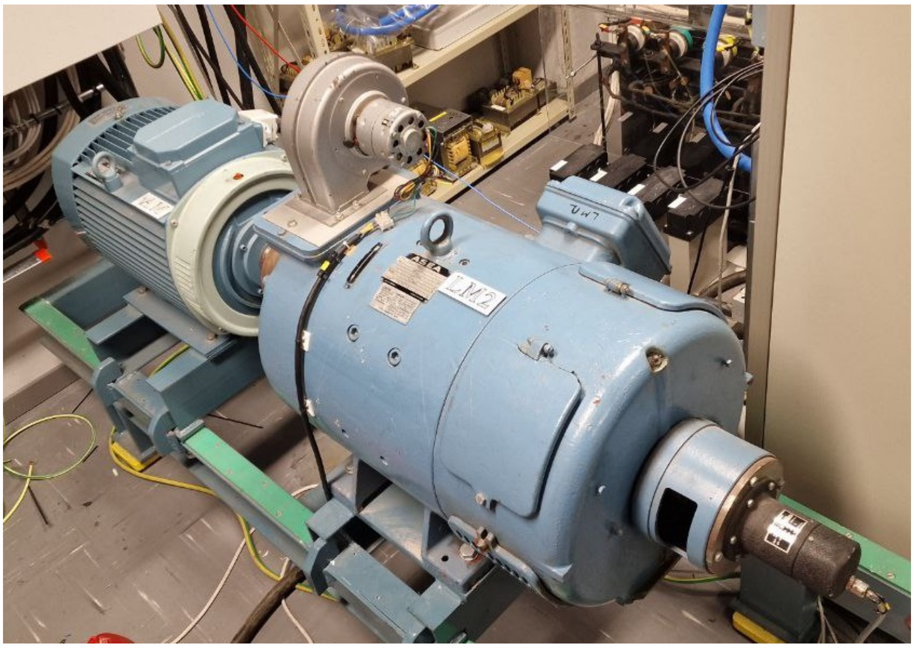

Figure 4.5: Induction machine

5

Test results

5.1 Lamp tests

5.1.1 5.5W Lamp set

As it was mentioned above the set of 3 lamps of 5.5W were connected in parallel and using the ACS.TSC equipment the lamp setup was tested. Tests with the sampling frequency of 5kH of the equipment, which is t=2s, are shown below and they represent active power consumption of the lamps for each frequency. Power of the lamps were calculated using the IEEE standard calculation method. Active power is calculated by

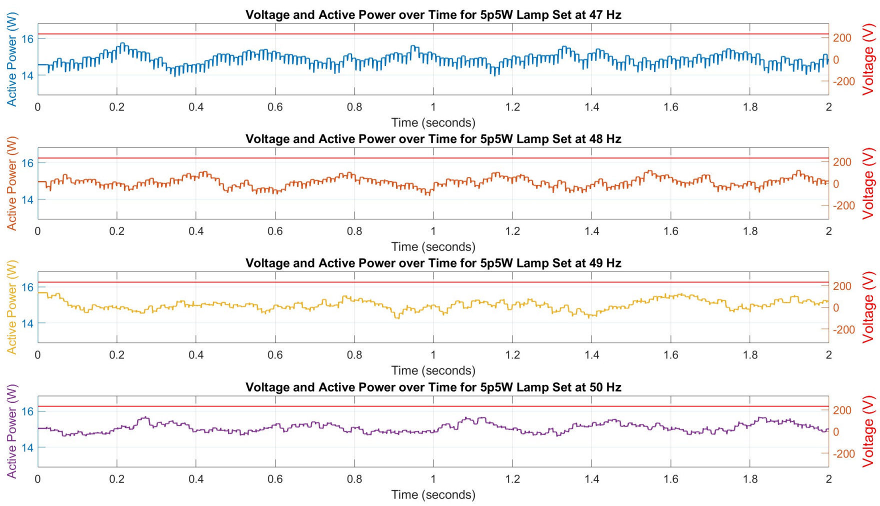

Figure 5.1: Active power for three 5.5W lamp set for 47-50 Hz

During the test of set of 5.5W lamps it was noticed that with the change in frequency active power varies across the time. The active power waveforms are similar to those which were reviewed Section 1. As it is seen in the figures there is a small fluctuation in the power lines. With the constant voltage, it can be assumed that the lamps behave differently at abnormal frequency values. For 50 Hz frequency the power line is more stable and for 47Hz and 53Hz the ripple is higher than others.

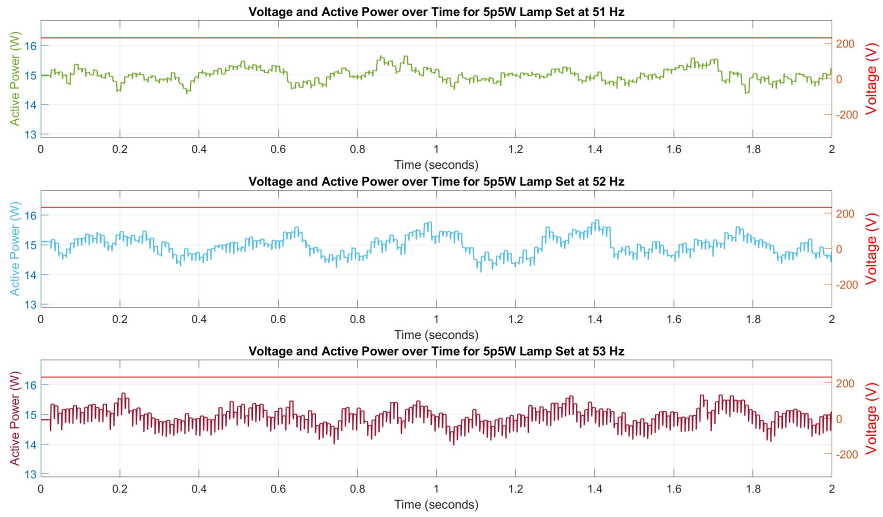

Figure 5.2: Active power for three 5.5W lamp set for 51-53 Hz

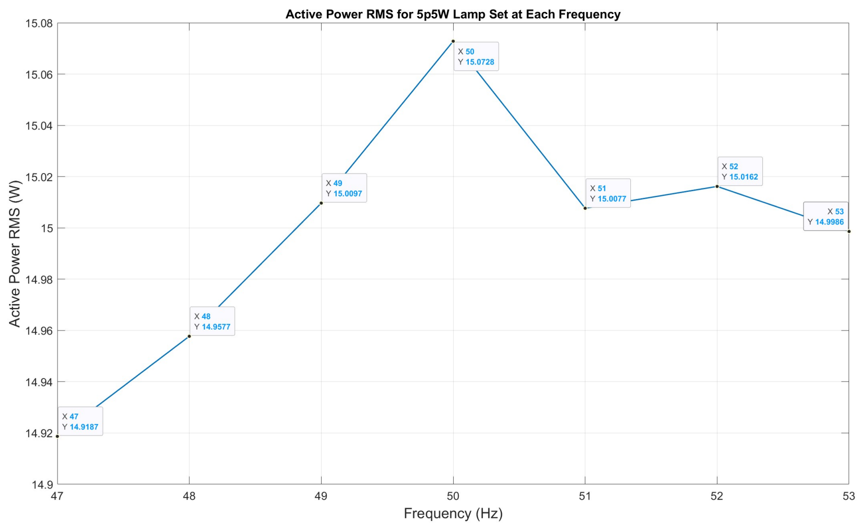

Figure 5.3: Three 5.5W lamp set RMS Active power

The RMS values of the active power represented below show the deviations in active power with each frequency. The behavior of the lamps from this manufacturer behave linear from the 47-50Hz, starting from the lowest power measurement of 14.92W to its peak measured power of 15.07W. With the change in frequency to 51Hz and above, the measured values are varied around 15W and illustrates steady-state values.

Mainly the reactive power variations are related to the change in voltage, so for the frequency deviations the reactive power change will be low. However, it is observed that there is a ripple for the reactive power graph and it has the similar effect as it was for active power.

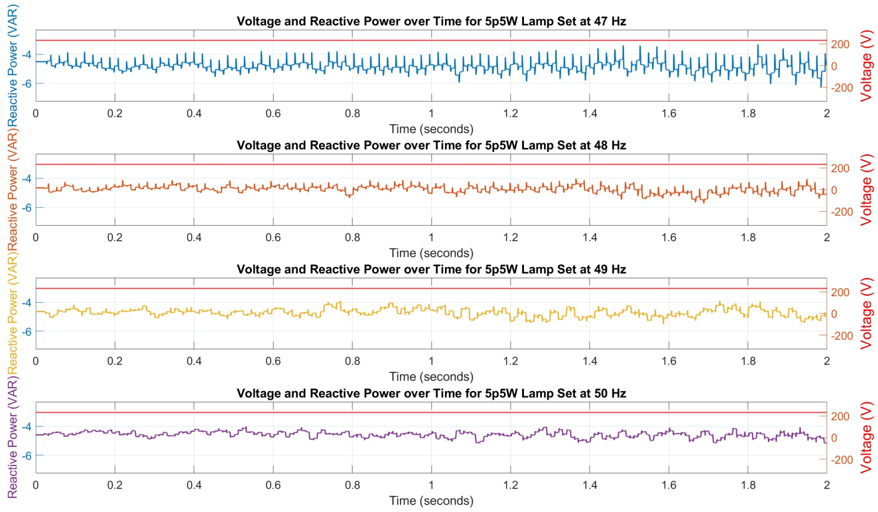

Figure 5.4: Three 5.5W lamp set RMS Reactive power for 47-50Hz

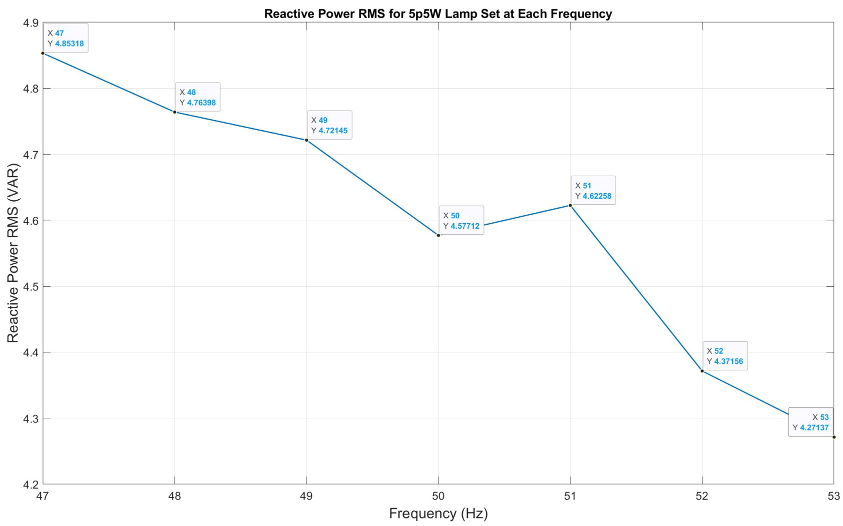

Figure 5.5: Three 5.5W lamp set RMS Reactive power

As it is seen from the Figure 5.5 the reactive power generated for 5.5W lamp set is around 4.5 VAR, but it should be noted that reactive power decreases with the change in frequency.

Table 5.1: Reactive power results for set of 5.5W lamps

Frequency	*Phase − lag*	*Type*
47 Hz	-16.92	Inductive
48 Hz	-17.28	Inductive
49 Hz	-17.64	Inductive
50 Hz	-14.40	Inductive
51 Hz	-14.68	Inductive
52 Hz	-14.97	Inductive
53 Hz	-15.26	Inductive

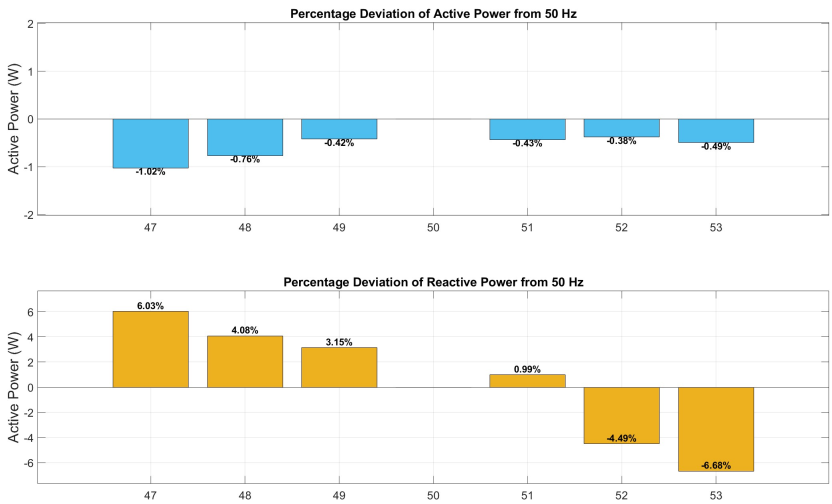

Figure 5.6: Percentage deviation of Active and Reactive power for abnormal frequencies

From the Figure 5.6 and Table 5.1 it is seen that the reactive power deviation is much higher for the lamp set. The active power varies for 1% at the maximum varied frequency, while reactive power has a deviation of 6% at 47Hz and 6.6% at 53 Hz.

5.1.2 7.5W Lamp set

Same test as for 5.5W lamp setup was implemented for 7.5W lamps. Figures below show active power for each frequency. The active power for the 7.5W lamp set more stable behavior compared with the 5.5W lamps. It can be noted that with shifting the frequency from the nominal frequency the power ripple increases in magnitude and at 50Hz the power output is almost stable.

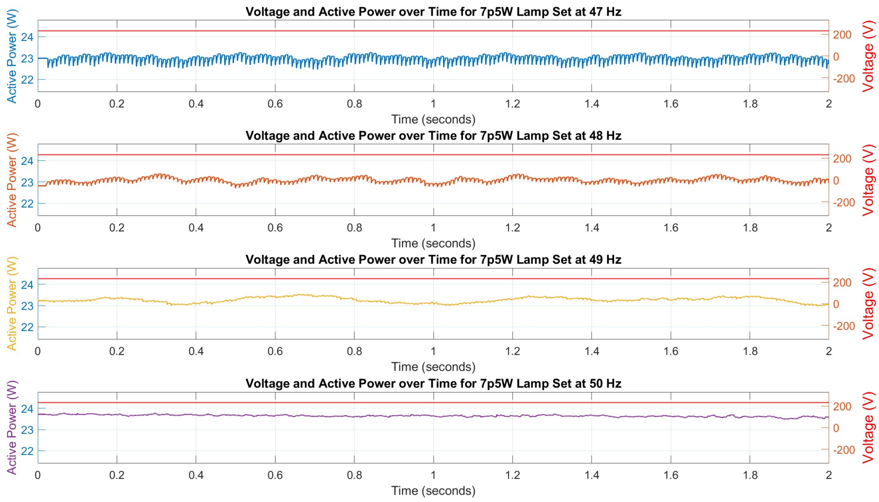

Figure 5.7: Active power for three 7.5W lamp set for 47-50 Hz

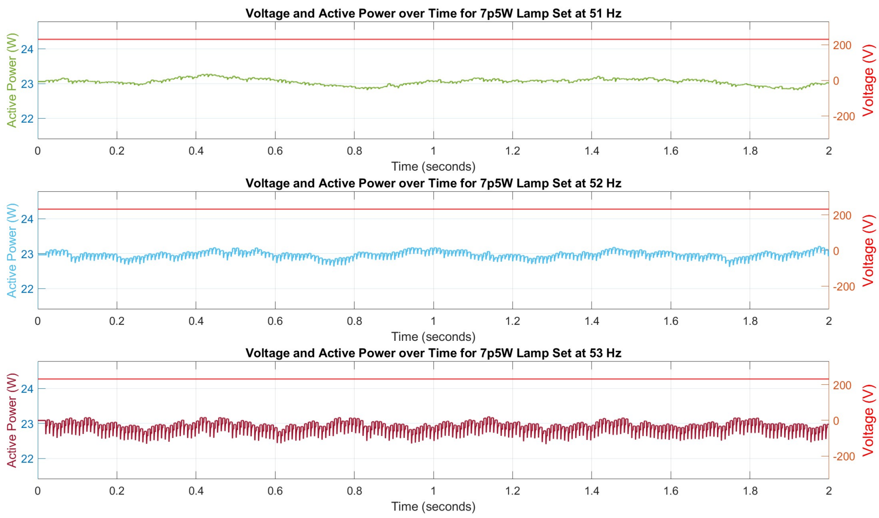

Figure 5.8: Active power for three 7.5W lamp set for 51-53 Hz

According to the RMS power values for this setup there is a non-linear trend. For 50Hz there is a peak value of active power and for the highest variation in the study, at 53Hz the power value is the lowest. It also can be noted that there is a rapid change in power consumption when the frequency is changed from 50Hz to 51Hz. When it comes to a reactive power for the lower frequency values this set of lamps shows steady values. However, the peak reactive power appear at 50Hz and significantly decreases at 51Hz, same as for active power.

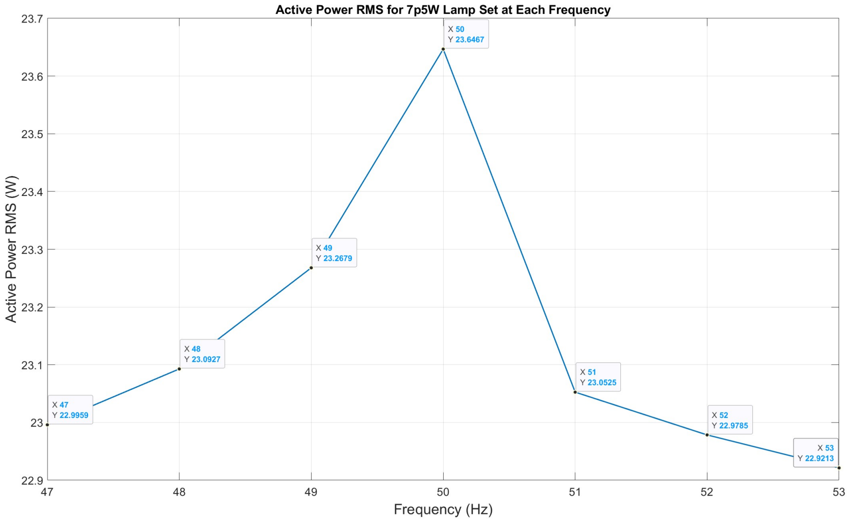

Figure 5.9: Three 7.5W lamp set RMS Active power

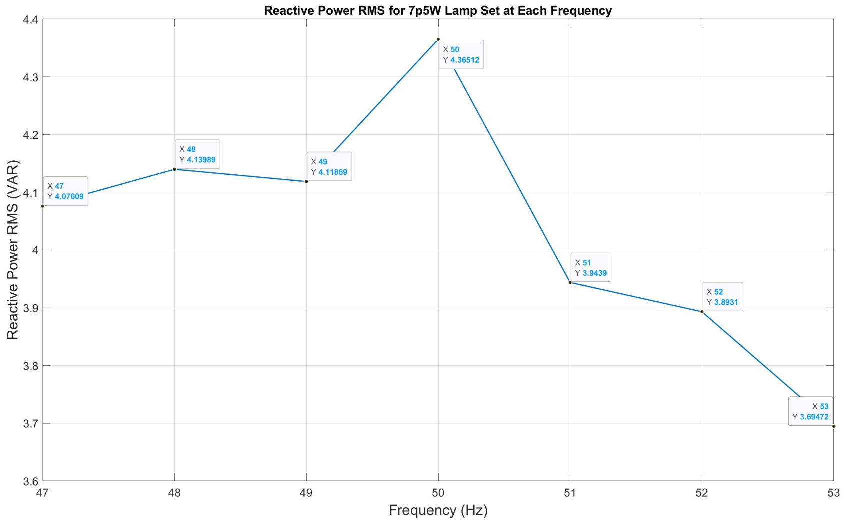

Figure 5.10: Three 7.5W lamp set RMS Reactive power

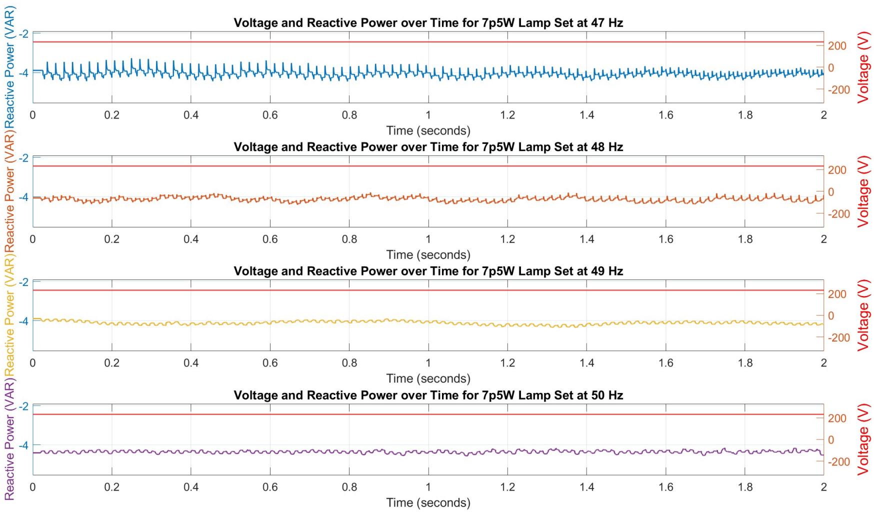

Figure 5.11: Three 7.5W lamp -set Reactive power for 47-51 Hz

According to the reactive power waveforms for this lamp set it can be noticed that for bottom line frequency the ripple is high. From the measured voltage and current the phase-lag between these two can be calculated. Table 5.2 shows the calculated phase-lag and indicates the reactive power for this test.

Table 5.2: Reactive power results for set of 7.5W lamps

Frequency	*Phase − lag*	*Type*
47 Hz	-10.15	Inductive
48 Hz	-10.37	Inductive
49 Hz	-10.58	Inductive
50 Hz	-10.80	Inductive
51 Hz	-11.02	Inductive
52 Hz	-7.48	Inductive
53 Hz	-7.63	Inductive

5.1.3 9.5W Lamp set

The study of 9.5W lamp set is the similar with the mentioned above. It can be seen from the Figure 5.9 and Figure 5.10 that the larger the frequency variations larger the ripple in active power consumption. Also, for this setup it is noticed that at the nominal frequency, 50Hz, active power waveform has the largest fluctuations among the studied cases.

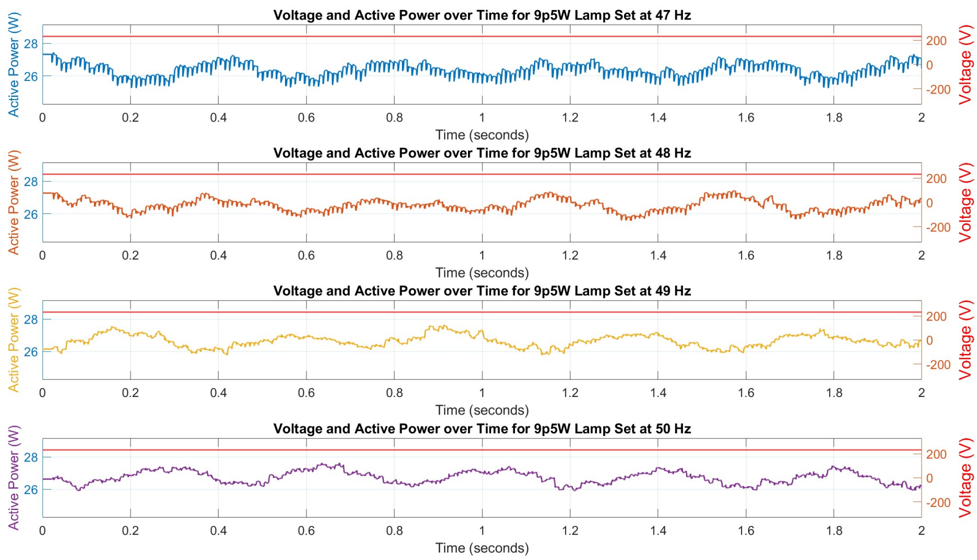

Figure 5.12: Active power for three 9.5W lamp set for 47-50 Hz

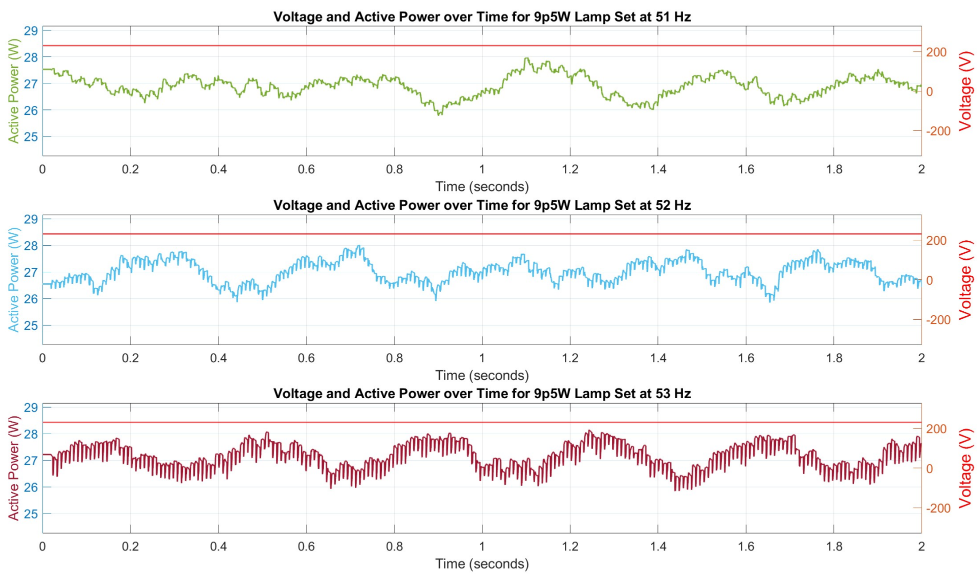

Figure 5.13: Active power for three 9.5W lamp set for 51-53 Hz

According to the RMS values this setup's active power consumption at 53Hz is higher and more stable than those for other frequency values. It shows the linear trend and with the frequency increase there is an increase in active power consumption. From the Figure 5.12 it is seen that the reactive power is not showing the linear behavior as active power. Also, there is a significant reactive power consumption of the lamp set with the peak value of 18.3 VAR.

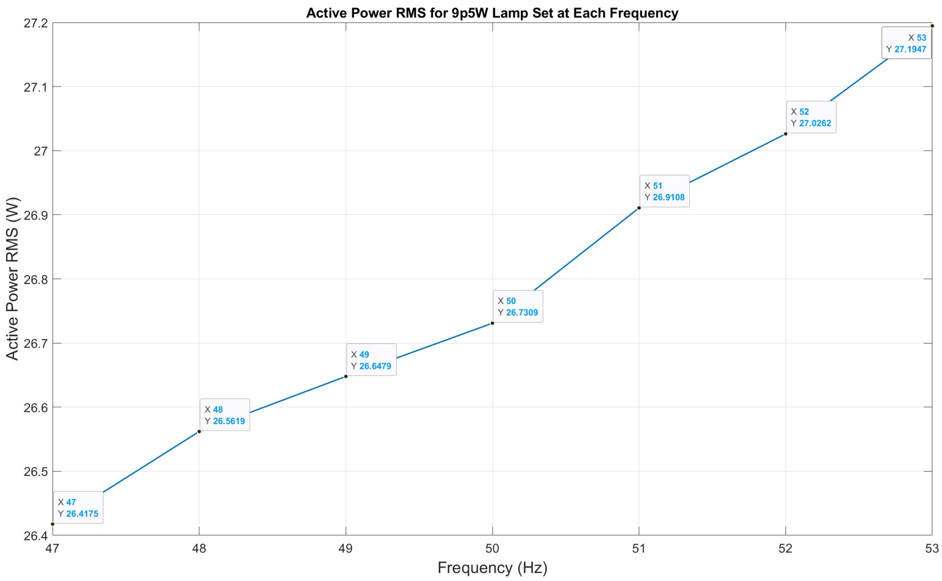

Figure 5.14: Three 9.5W lamp set RMS Active power

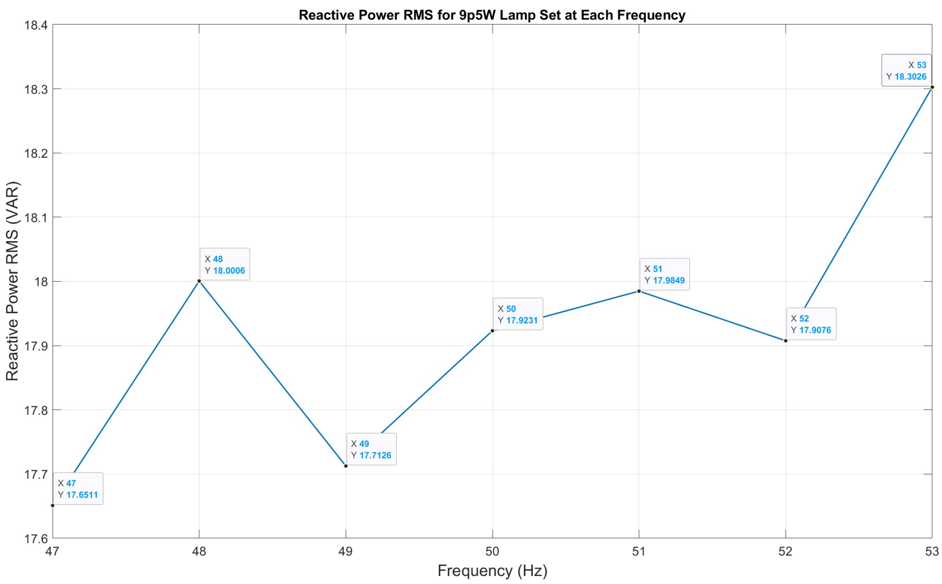

Figure 5.15: Three 9.5W lamp set RMS Reactive power

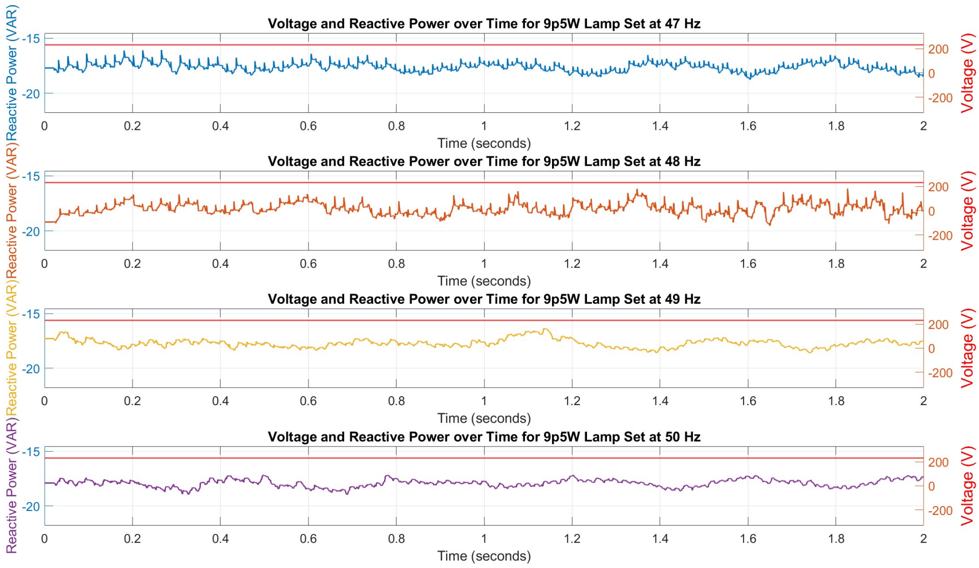

Figure 5.16: Reactive power for each frequency for 47-51Hz

Studying the reactive power waveforms it can be identified whether the reactive power is inductive or capacitive. With the help of MATLAB the phase-shift is calculated and stated in the table below. As it is seen from the table reactive power is inductive for this test.

Table 5.3: Rated and measured active power for the lamps

$Frequency$	$Phase - lag$	$Type$
47 Hz	-33.84	Inductive
48 Hz	-34.56	Inductive
49 Hz	-35.28	Inductive
50 Hz	-32.40	Inductive
51 Hz	-33.048	Inductive
52 Hz	-33.69	Inductive
53 Hz	-34.34	Inductive

5.1.4 All lamps combined

Combination of all three sets is also studied and it is helpful in comparing the laboratory experiments with the real-life cases. For the results of this test the similar pattern can be observed, discrepancy in top and bottom line of frequency results in larger ripple in active power. It can be also noted that combining all the lamps together leads to to fluctuations similar to those in 9.5W and 5.5W lamp sets.

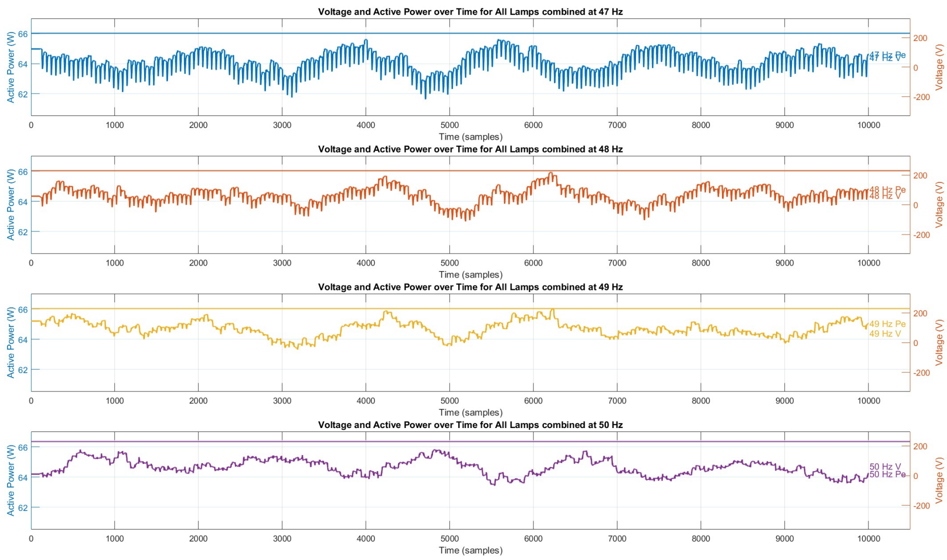

Figure 5.17: Active power for All lamps for 47-50 Hz

Figure 5.18: Active power for All lamps for 51-53 Hz

Looking at Figure 5.15 it can be observed that the active power within the 47-53Hz behaves non-linearly. For the first 3 frequency values there is a linear behavior, but after 49Hz active power declines. Also, around the nominal frequency 49-51Hz are in a close range. At 53Hz the active power is the lowest among the measured values. For the reactive power represented in Figure 5.16 from 47Hz to 51Hz measured values are in close range and after it declines significantly.

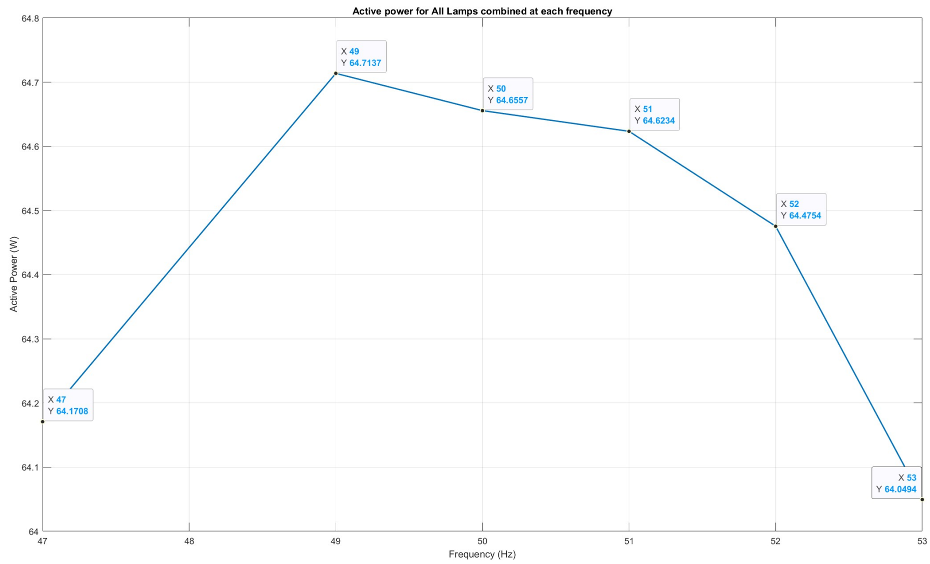

Figure 5.19: All lamps RMS Active power

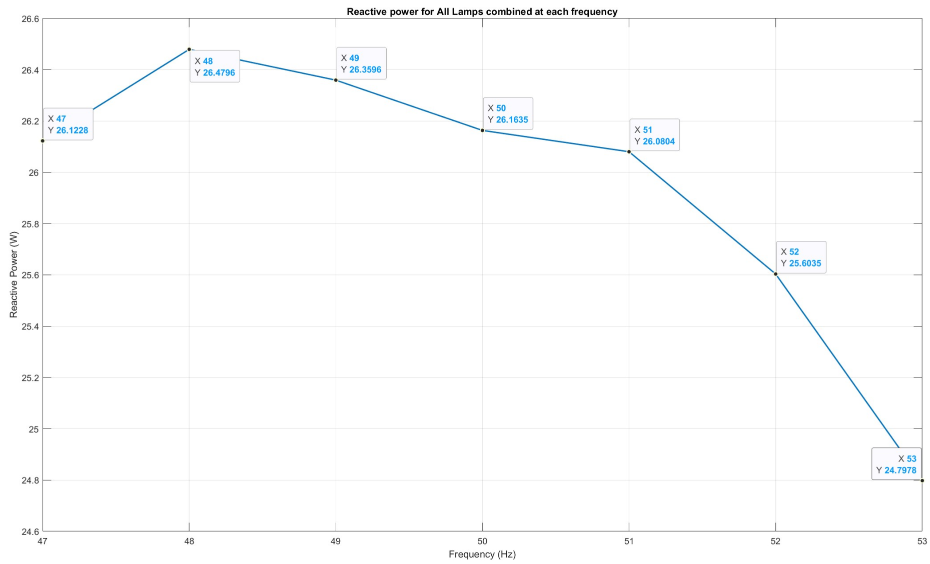

Figure 5.20: All RMS Reactive power

5.2 Electric heater

For the heater with the fan on the same procedure was held with the constant voltage supply from ACS.TCS Regatron. It is noticed that with varying frequency the active power ripple is increasing. There is a symmetric effect, a similar pattern for the active power ripple in a direction furthest to nominal. It is observed that at 50Hz there is almost no ripple and the power waveform of the heater is stabilized.

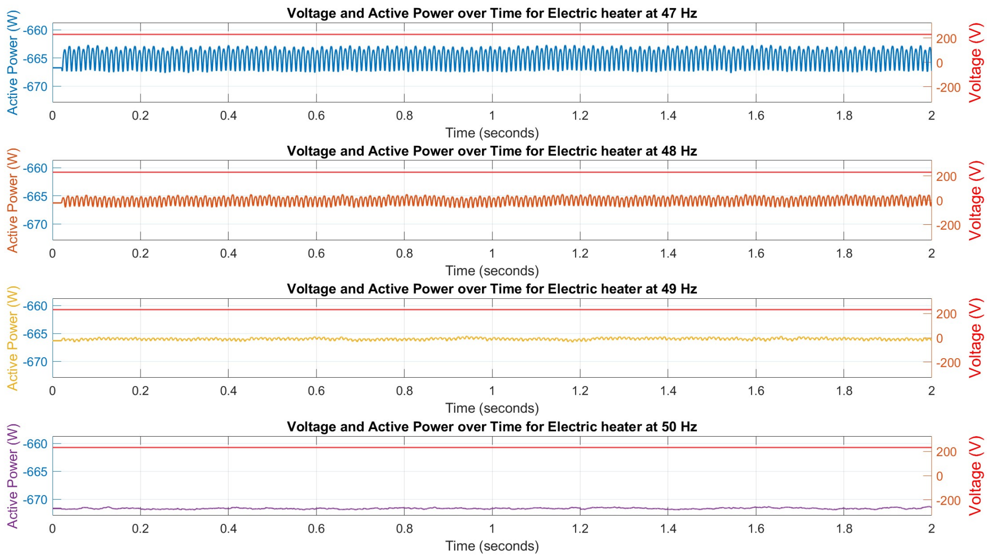

Figure 5.21: Active power for Heater test for 47-50Hz

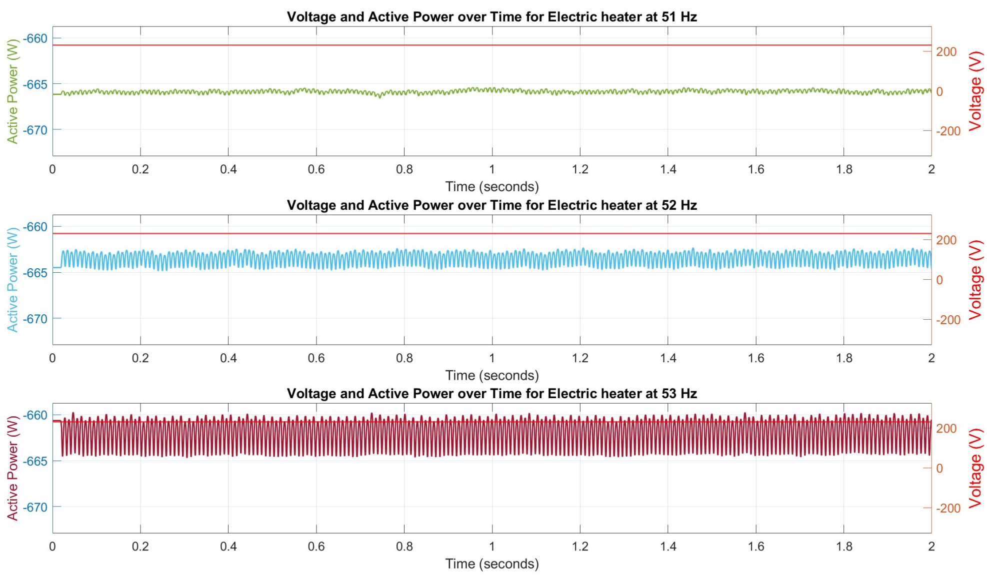

Figure 5.22: Active power for Heater test for 51-53Hz

One of the reasons for the power ripple changes us the fan. Under varying frequency speed of fan changes and then it affects the power consumption.

From the Figure 5.25 it is observed that the active power consumption of the heater has very small variation. With the highest peak value of 671.65W and with the lowest peak of 661.94W, power variation is 10W. Also it can be seen that the peak value appears at 50Hz, which means that it is the rated frequency for this equipment.

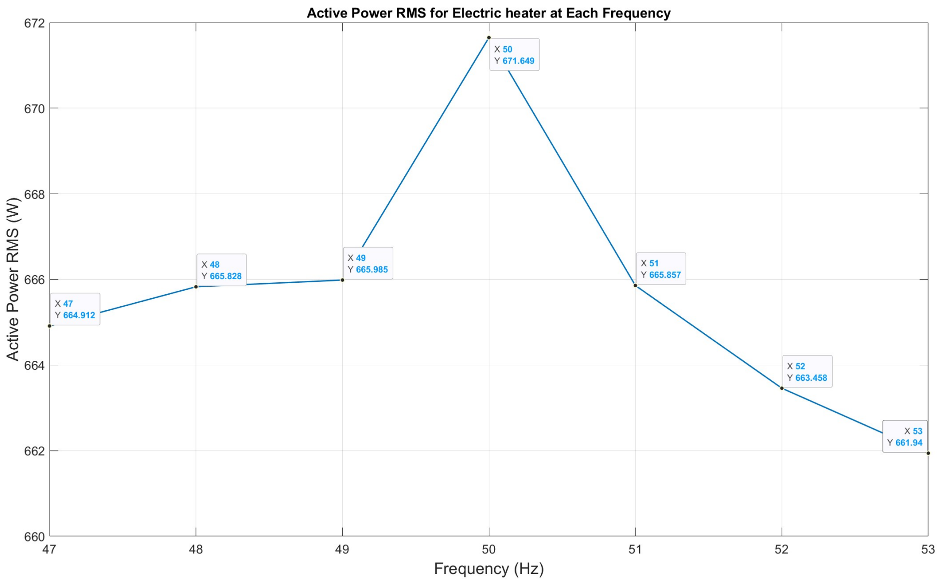

Figure 5.23: Active power RMS for Heater at each frequency

5.3 Induction machine

5.3.1 7.5kW loading

For the three-phase induction motor laboratory experiment, synchronous machine was used as a controllable power supply. The first test is with 7.5kW loading of induction machine and active power for different frequencies are measured. From Figure 5.17 and Figure 5.18 the active power varies a lot for this simulation. With lower loading the rotational speed of IM is higher.

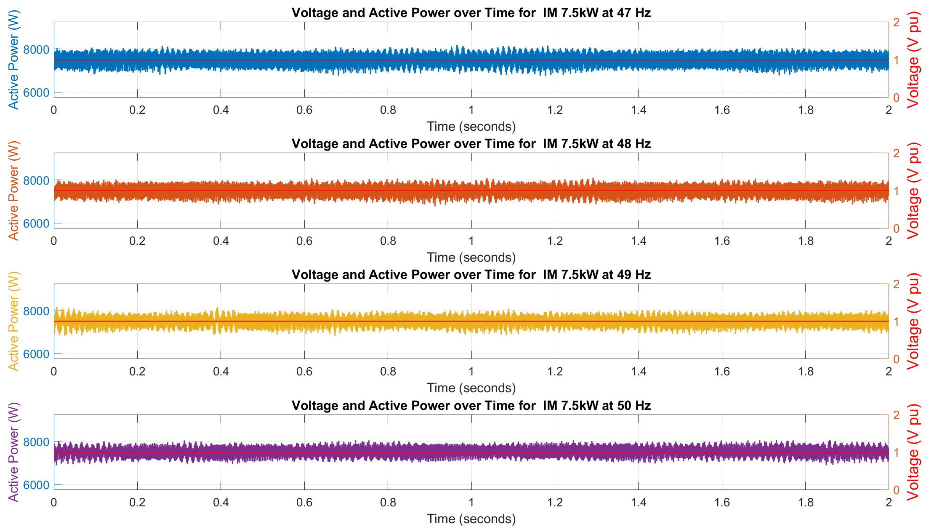

Figure 5.24: Active power for 7.5kW IM test for 47-50Hz

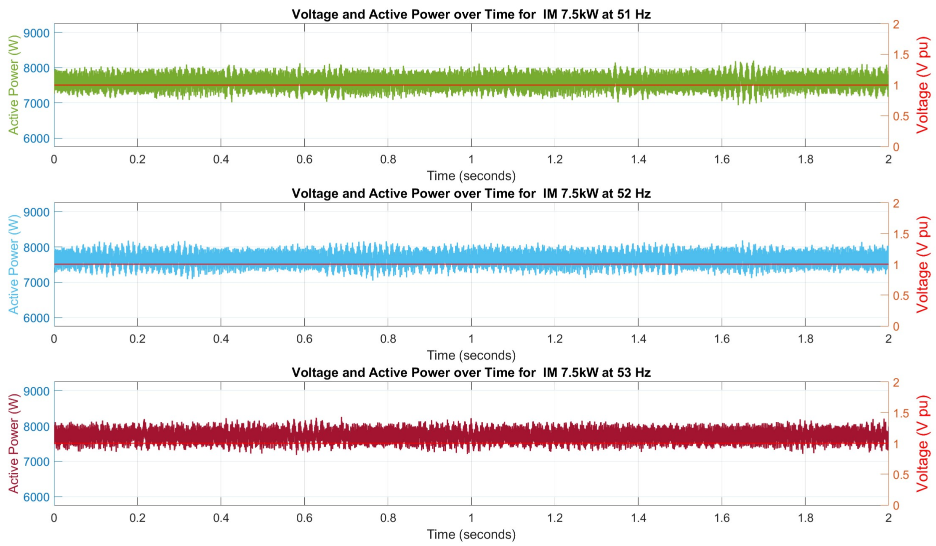

Figure 5.25: Active power for 7.5kW IM test for 51-53Hz

According to the RMS values of 7.5kW IM loading the power variation is not much. For under-frequency occasions the active power is around 7.5kW and it is almost the same for 47-49Hz. At 50Hz frequency IM has its rated power and for over-frequency cases active power starts to increase.

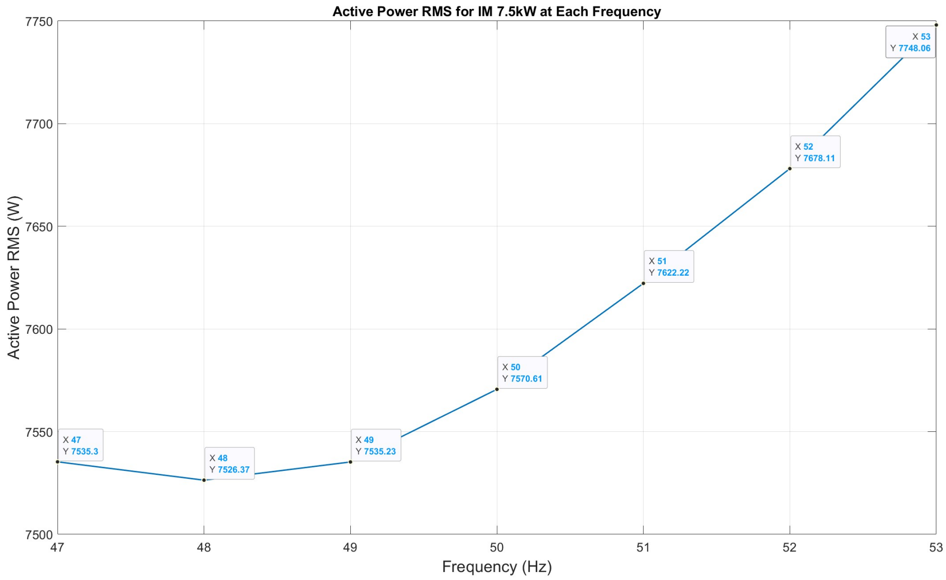

Figure 5.26: Active power RMS for 7.5kW Induction machine at each frequency

For the IM test reactive power should be also observed. For this test reactive power of IM was measured for each frequency variation and displayed on Figures 5.26-27.

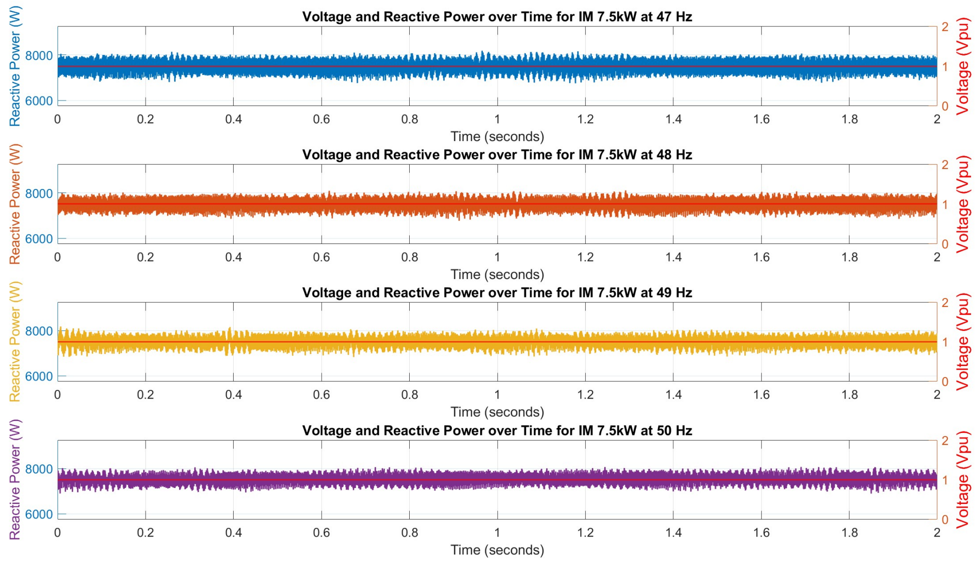

Figure 5.27: Reactive power RMS for 7.5kW Induction machine for 47-50 Hz

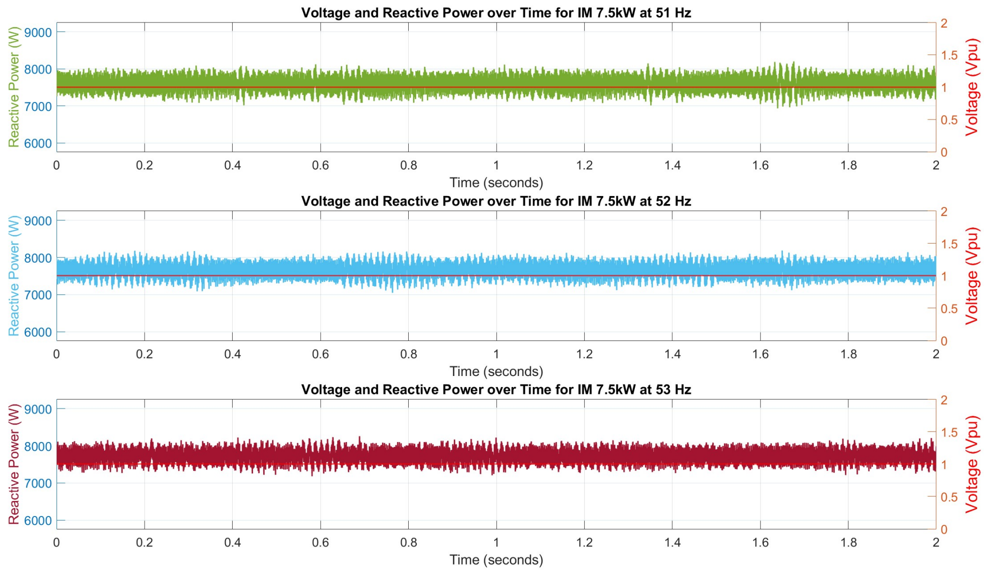

Figure 5.28: Reactive power RMS for 7.5kW Induction machine for 51-53 Hz

From these figures it is seen that for nominal frequency reactive power has less ripple than the reactive power measurements for the bottom line and top line frequency variations. Also, from the RMS reactive power graph it is seen than with increasing frequency reactive power is decreasing.

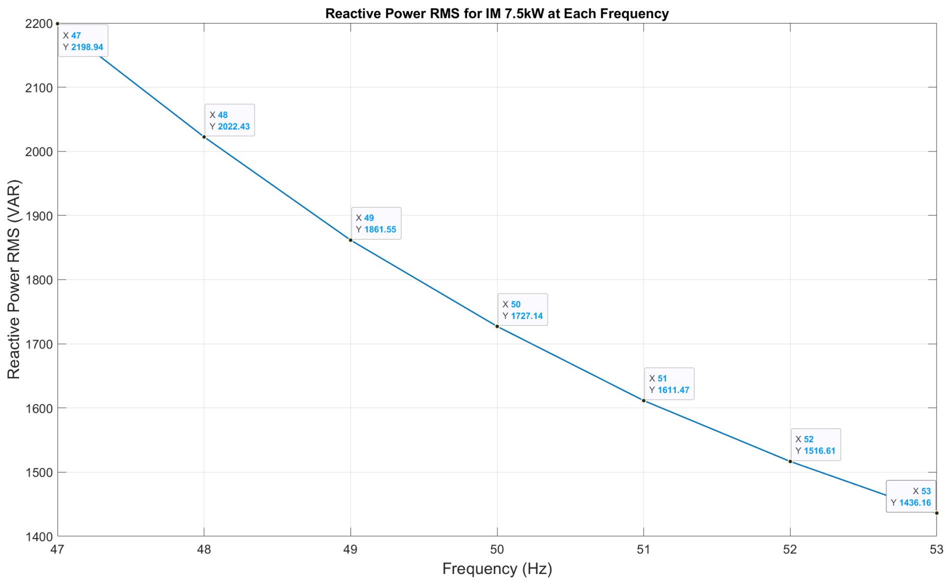

Figure 5.29: Reactive power RMS for 7.5kW Induction machine at each frequency

5.3.2 15kW loading

For the 15kW IM loading has the same active power pattern for different frequencies as it has been noted for 7.5kW IM loading. From Figure 5.20 and Figure 5.21 it is seen that measured active power is as rated active power. The difference from the previous case is that active power waveforms vary less. With higher loading the inertia will be larder and rotational speed of machine will be lower.

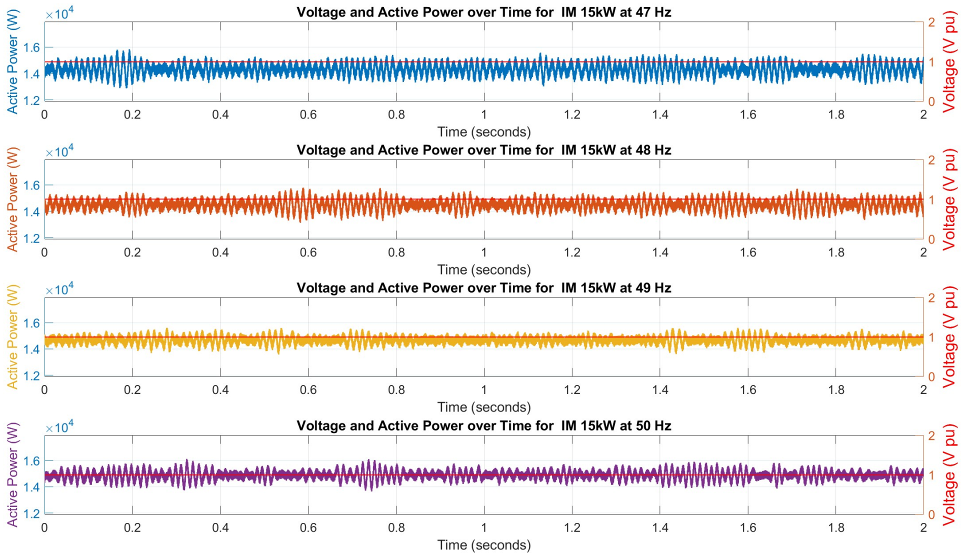

Figure 5.30: Active power for 15kW IM test for 47-50Hz

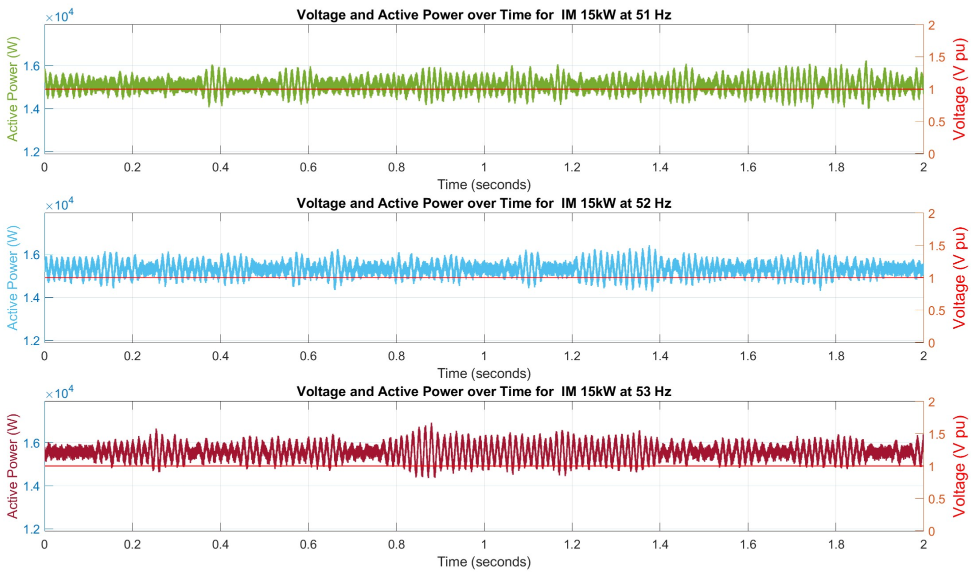

Figure 5.31: Active power for 15kW IM test for 51-53Hz

According to the RMS active power measurements for 15kW loading for all the frequency values there is a linear trend. With lower frequency consumed active power is less and vice versa. It is also seen that active power variation is comparatively low. At 50Hz measured active power is close enough to the rated power.

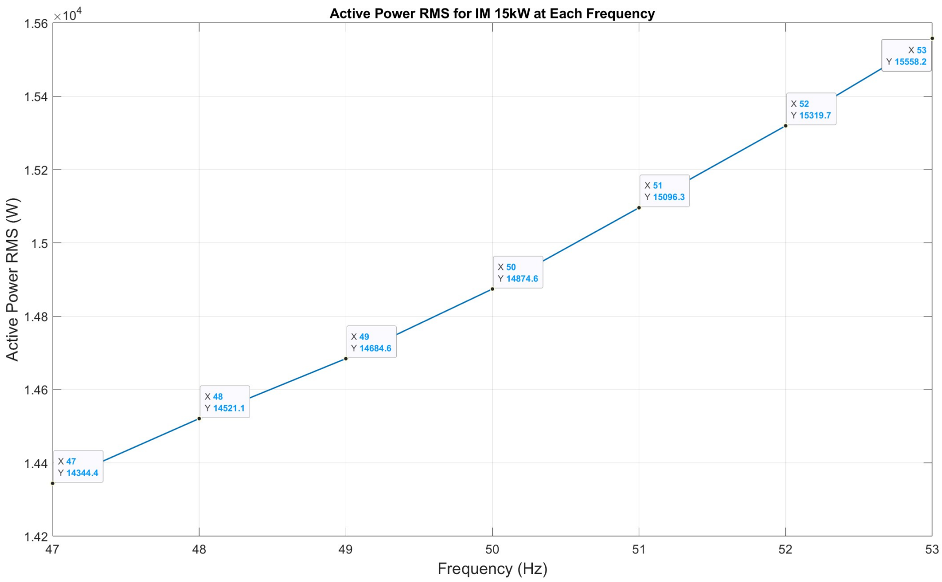

Figure 5.32: Active power RMS for 15kW Induction machine at each frequency

As it was seen for the previous test the measured reactive power behaves the same as the active power measurements. For the 50Hz operation reactive power is with smaller ripple.

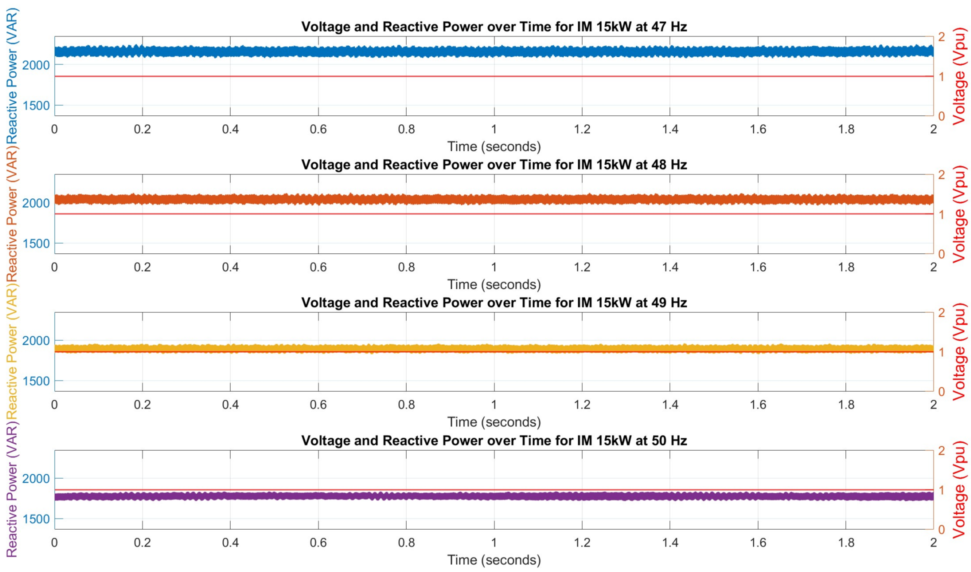

Figure 5.33: Reactive power RMS for 15kW Induction machine for 47-50 Hz

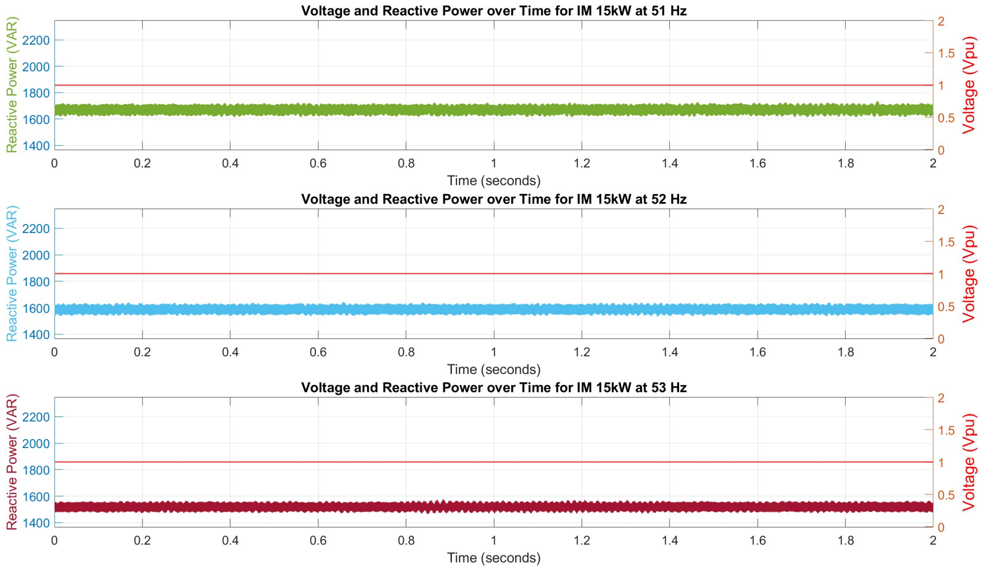

Figure 5.34: Reactive power RMS for 15kW Induction machine for 51-53 Hz

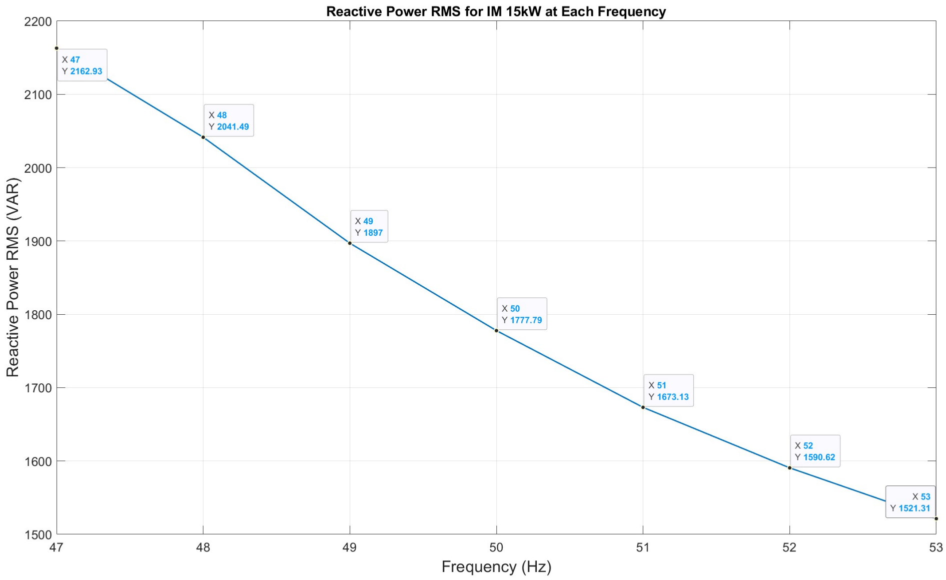

Figure 5.35: Reactive power RMS for 15kW Induction machine

6

Analysis & Discussion

6.1 Lamp test

During this study several cases of the lamps sets were examined and different patterns of active power consumption were noticed. For the 5.5W lamp setup it was found that measured power values are lower than the rated power for all the frequency values. It is similar with the 9.5W setup. The power variations for this tests were calculated and represented in Table 6.1.

Table 6.1: Rated and measured active power for the lamps

Setup	*Rated*	*Meaured[Max]*	*Meaured[Min]*	*Deviation*
5.5W setup	16.5	15.0728	14.9187	-9.58%
7.5W setup	22.5W	23.6467	22.9213	5.09%
9.5W setup	28.5W	27.1947	26.4175	-7.31%
Combined	67.5W	64.7137	64.0494	-5.1%

From this table it can be seen that for the 5.5W and 9.5W lamp setups the deviation of measured power from the expected power consumption is -9.58% and -7.31% respectively. It means that these lamps consume less power than it was stated by the manufacturer. For the 7.5W lamp setup there is a positive deviation of 5.09%, which means that it consumes more power than it was stated. However, in small scale applications this error is not significant and will not have influence on power system. Also, for the combination of all lamps was the simulation of the real-life scenario, hence this results may illustrate the close values. When combining all lamps together the deviation from the expected power was -5.1%, which is set by majority of the lamps with similar trend.

The Figure 6.1 represents the circuits and Figure 6.2 shows the components of the tested lamps. There are different components for each of the lamps, but close look reveals that 5.5W has a simple circuit with one output capacitor bank. It was noted that 7.5W lamps have additional components, which were not identified, but they were assumed to be a MOSFET used for switching applications and output voltage regulator. For 9.5W lamps a Step-Down Driver was used in the input and several capacitors and inductors are seen in the circuit.

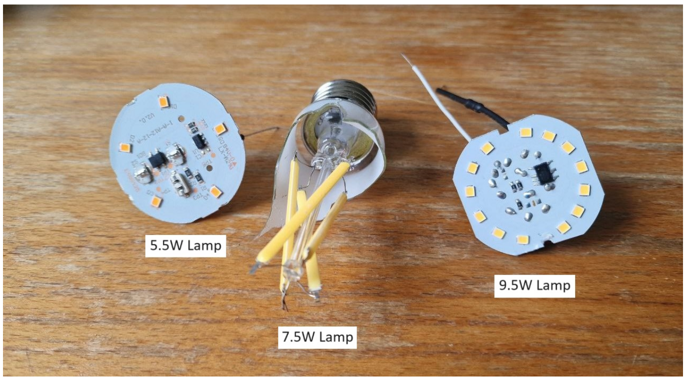

Figure 6.1: Circuits for each of the lamps

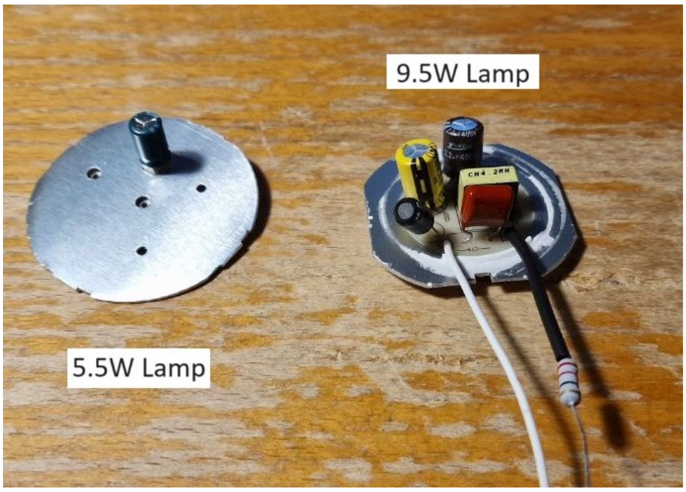

Figure 6.2: Components of different lamps

The key point for lower power LED is that the diode bridge rectifier is enough to regulate the input voltage ripple and still meet the electric performance. It is similar for 5.5W and 7.5W lamps, and the RMS active power pattern was similar for these sets. As it was stated in literature review simple rectifiers are more suffered to voltage and current ripples. The difference in more complex circuit for 7.5W lamps gives contrast in output current and voltage ripples.

A Step-Down Driver used in 9.5W lamp is also be affected by abnormal frequencies of input voltage. That is why its circuit is more complex and has much more components than others. Capacitors smooth out the DC voltage, while inductors filter and stabilize the current. The Step-Down Driver on the LED board maintains a constant current to the LEDs, shielding them from fluctuations and ensuring even brightness. By integrating these components, the circuit guarantees that the LEDs function efficiently and maintain consistent brightness.

6.1.1 Frequency dependence of the lamps

Considering the RMS values of the active power for all the tests it is seen from the Figure 6.3 that the changes in active power consumption are not significant. Recalling the graphs of RMS active power for each of setups the change in active power is within the range of 5%. According to the hypothesis in literature review, LED lighting load is considered as a resistive load model and it is independent of the frequency variations.

Table 6.2: Variations of measured active power

Setup	*Meaured[Max]*	*Meaured[Min]*	*Variation*
5.5W setup	15.0728	14.9187	1.1%
7.5W setup	23.6467	22.9213	3.1%
9.5W setup	27.1947	26.4175	2.8%
Combined	64.7137	64.0494	1.1%

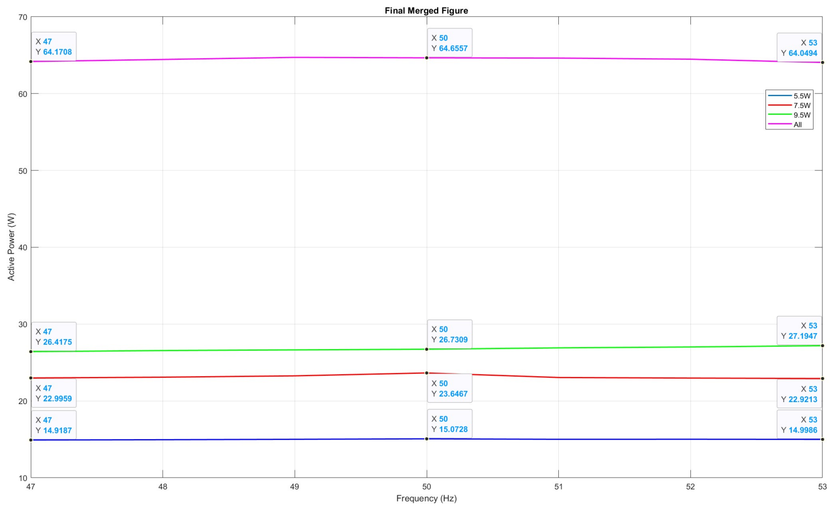

Figure 6.3: Active power RMS for All Lamps at each frequency

As it was stated in theory part, lamps frequency sensitivity coefficients can be calculated. Table 6.3 shows the coefficient for different lamps. As it can be seen from the table the K_{Pf} for the lamps are very low, they are in 10^{-3} scale. It should be also noted that the highest K_{Pf} corresponds to the 7.5W lamp and this lamp set was showing the more active power consumption than rated.

Table 6.3: Variations of measured active power

Coefficient	$5.5W set$	$7.5W set$	$9.5W set$
K_{Pf} [1/Hz]	0.00155	0.00537	0.00454
K_{Qf} [1/Hz]	0.00587	0.00496	0.00381

6.2 Induction machine tests

Two tests were proceeded for the Induction machine frequency dependence. According to the Figure 6.4 it is seen that for 7.5kW and 15kW loading there is a increasing trend. For higher loading the rate of change is higher, which is proportional to the loading of IM. Using the Equation 2.15 in section 2 a frequency dependence of IM can be derived.

1. IM Frequency dependence

$$P_e = T_e * \omega_m \tag{6.1}$$

$$\omega_m = \omega_s * (1-s) * \frac{2}{p_f}, \therefore \omega_s = \frac{\omega_m * p_f}{2(1-s)} \tag{6.2}$$

$$P_e = \frac{3}{2}\frac{\omega_m * p_f}{(4\pi * f + \omega_m * p_f)} {I_r}^2 * R_r \tag{6.3}$$

-where ω_s is the angular velocity of stator, $\omega_m istheangularvelocityofrotor$,fisthe$frequency$,$p_f$ is the number of poles, and s is the slip.
From this equations the relation of change of power to change of frequency could be found. Taking the derivative of power over frequency gives the next equation. Equation 6.4 shows that the change of power is proportional to the change of frequency.

$$\frac{\Delta P}{P} \approx \frac{\Delta f}{f} \tag{6.4}$$

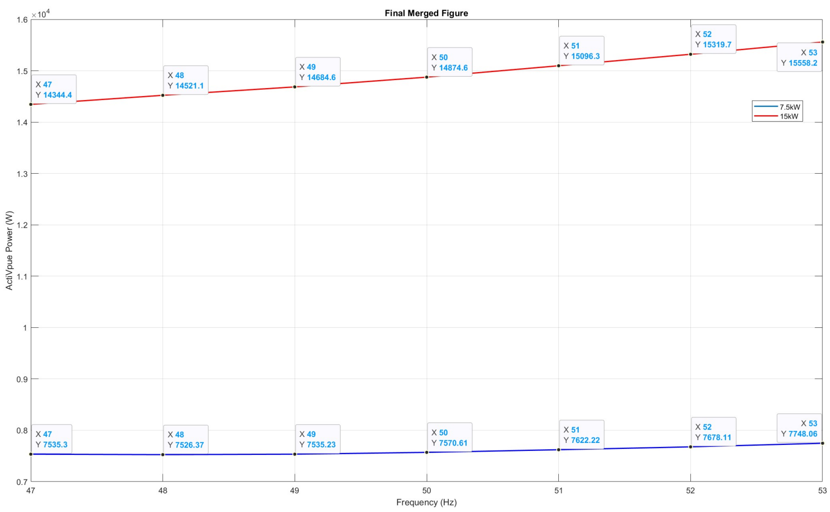

Figure 6.4: Active power for IM loading

From the Table 6.4 it is seen how the measured active power is varied for each loading. For 7.5kW loading measured power is varied for 2.9% and for 15kW loading

Table 6.4: Variations of measured active power

Loading	*Meaured[Max]*	*Meaured[Min]*	*Variation*
7.5kW load	7748.06	7526.37	2.9%
15kW load	15558.2	14344.4	7.8%

variation is 7.8% .

Table 6.5: Rated and measured active power for the IM

Setup	*Rated*	*Meaured[Max]*	*Meaured[Min]*	*Deviation*
7.5kW load	7500	7748.06	7526.37	3.3%
15kW load	15000	15558.2	14344.4	4.4%

The Table 6.5 shows the deviation of active power for the IM. It is apparent from the data that change in frequency does not affect the active power consumption. According to the NEMA MG1-12.42 Standards [25] a frequency variation of 5% is acceptable and these changes make IM suited to variety of applications. For these tests a frequency variation of 6% was implemented. There is an effect of frequency on IM, but it has a linear trend as it was stated in the standards.

A power deviation graph was drawn to show the deviation from the nominal 50Hz operation. There are 2 graphs for 2 tests of Induction machine. Overall, it is seen that both tests have the same patterns in deviations. As it is seen from the Figure 6.5 the active power has more stable deviation from the nominal operation frequency. For the reactive power the deviation from 50Hz operation is significant for 7.5kW loading.

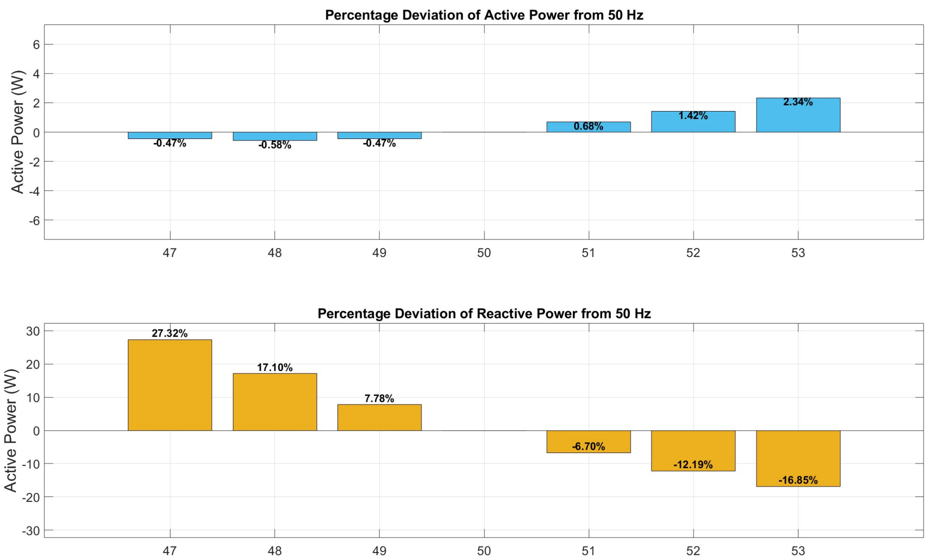

Figure 6.5: Percentage of the deviation for 7.5kW loading

Figure 6.6 represents the percentage deviation form the nominal frequency operation for 15kW loading of IM. From this figure it is seen that active power deviation is within the 5% margin, but for the reactive power in the same manner as for 7.5kW loading deviation is much more.

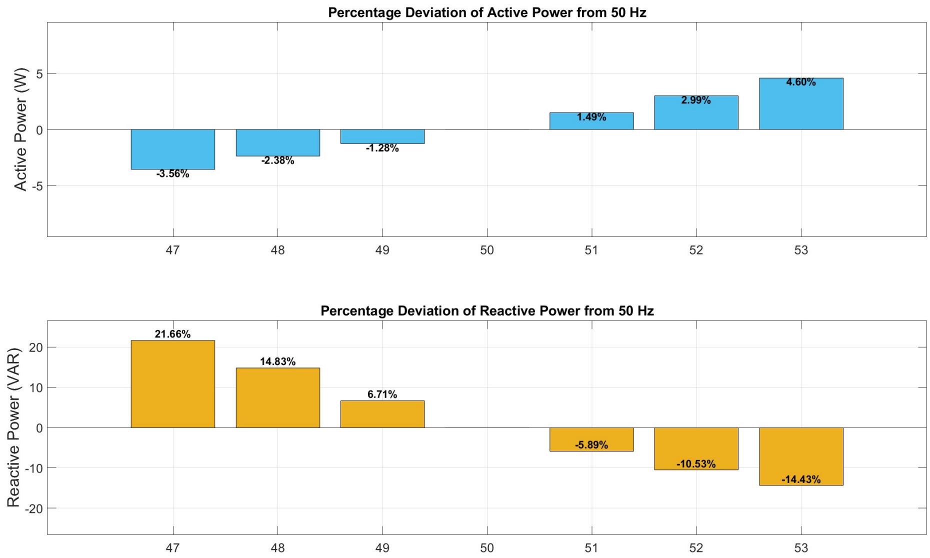

Figure 6.6: Percentage of the deviation for 15kW loading

6.3 Electric heater

For this study electrical heater was not used at its full power. Adjusting the temperature controller it was estimated that the rated power is 800W. Electrical heater used in this study represented expected outcome of the experiments. Direct-resistance heater showed the small frequency fluctuations compared to other load models used in this study.

Table 6.6: Rated and measured active power for the lamps

Setup	*Estimated*	*Meaured[Max]*	*Meaured[Min]*	*Variation*	*Deviation*
Heater	800	671.65	661.94	1.4%	16.5%

As it is seen from the Table 6.6 the measured active power variation is at 1.4% and those variations are really close to each other. Also it should be noted that the measured power is lower than rated by 16.7%. This deviation shows that the power dissipation is high for resistive heater. It is reasonable because as it was stated in [9] there are radiation losses and convection losses from the surface of resistor.

6.4 Ethics & Sustainability

An important ethical aspect relevant to this project defined by IEEE code of Ethics is to uphold the highest standards of integrity, responsible behavior, and ethical conduct in professional activities.

During the thesis, it was ensured that all data collected during the investigation of frequency dependency on LED lamps, induction machines, and electrical heaters was accurate and thoroughly validated. Any potential deviations or uncertainties in the data were clearly communicated, preventing the dissemination of misleading or inaccurate results. This approach upheld the principles of integrity and transparency in reporting, which are essential to both academic research and the practical applications of the findings.

As power loads such as LED lamps, induction machines, and electrical heaters are widely used across residential, industrial, and commercial sectors, the findings from this research have the potential to impact a broad range of users. The research is conducted with a focus on promoting fairness and ensuring that any benefits arising from the work are distributed equitably. Additionally, it aims to ensure that technological advancements contribute to improving quality of life without exacerbating existing inequalities.

From sustainability aspect, by understanding the frequency dependency of these power loads, the research can contribute to increasing the longevity and reliability of the equipment. Prolonging the lifespan of devices like LED lamps and induction machines reduces the need for frequent replacements, thus conserving resources used in the production, transportation, and disposal of these devices. This is particularly important in the context of sustainable manufacturing and minimizing the environmental impact of electronic waste.

7

Conclusions and Future work

7.1 Conclusions

This thesis presents a frequency study of various load types using a component-based approach to analyze the electrical characteristics of individual loads. The research covers both resistive and inductive loads, focusing on commonly used applications. By investigating their behavior under abnormal frequency conditions, the study provides insights that will inform future research on load behavior in power systems.

The most unexpected results were found in lighting loads, particularly LED lamps. Power ripples and trend lines were obtained for different electrical circuits, revealing that simple, low-power LEDs exhibit a significant decrease in power consumption with high frequency variation. In contrast, higher power LEDs with more complex circuits showed stabilized behavior. This difference is attributed to the advanced components used by manufacturers in LED circuits to meet efficiency standards, which results in varying stability under abnormal conditions due to the switching components present in the lamps.

The induction machine analyzed in this study demonstrated the expected behavior, following a linear trend. It was confirmed that a 5% variation in frequency leads to active power consumption within the range specified by standards. However, the reactive power deviated significantly, reaching nearly 30% in both studies, a typical response for an induction motor. Frequency variations between 47-53 Hz did not show any decline in performance, and the only factor affecting the induction machine was the load, consistent with theoretical expectations.

The direct resistance heater, commonly used in both home and industrial applications, was also examined. The study found minimal power losses in the resistor and high efficiency for the heater. Although the estimated rated power deviation was higher than expected, more accurate results could be achieved with equipment offering better scaling precision.

Overall, this study highlights interesting trends in LED lamps, showing that the lack of standardized electrical circuits for LEDs leads to varied behavior among different lamps. While the individual characteristics of these components influence specific lamps, their impact on aggregated loads remains insignificant.

7.1.1 Future studies

Based on the findings of this study, several areas for future work can be suggested to expand the understanding of frequency-dependent behavior in power loads, with particular emphasis on sustainability, renewable energy sources (RES), and aggregated power system loads.

1. **RES integrated power system**
   As the number of RES increases the more varied frequency occasions will arise. The loads connected to the RES integrated systems could be studies in order to determine a real-life scenario. Future research could explore how frequency variations from renewable energy sources, such as wind and solar power, affect the performance of different types of loads, particularly LEDs, induction machines, and electrical heaters. Given that RES can introduce greater frequency fluctuations due to their intermittent nature, studying their interaction with power loads will help in developing more resilient systems. This could inform the design of more adaptive load components and smarter power management strategies to accommodate the variability introduced by renewable energy generation.
2. **Impact of separate loads on aggregated load behavior in power systems**
   While this study focused on the behavior of individual loads, future work should examine the behavior of aggregated loads in larger power systems under abnormal frequency conditions. Since the study found minimal impact from LED circuits on aggregated loads, further investigation should analyze the collective behavior of various load types (resistive, inductive, and lighting) under frequency variations. This could improve the modeling and simulation of power system loads, providing insights into how different loads contribute to overall grid stability and efficiency, especially in systems with a high penetration of RES.
3. **Frequency-dependent modeling for industrial loads**
   While this study examined residential loads like LED lamps and heaters, future research could expand to include industrial loads and their aggregated behavior under varying frequencies. Industrial systems are typically more sensitive to frequency variations, and understanding their impact on the overall power system is crucial for sustainability and energy efficiency. This could include investigating how frequency-dependent power losses in large-scale industrial heaters and motors can be minimized, leading to more efficient energy use in industrial sectors.

By addressing these areas, future research can contribute to the development of more sustainable, energy-efficient power systems capable of integrating high levels of renewable energy while maintaining grid stability and minimizing environmental impact.

Bibliography

[1] “Advances in Grid-Connected photovoltaic power conversion systems,” in Elsevier eBooks, 2019. doi: 10.1016/c2016-0-05033-7.

[2] R. Shah, N. Mithulananthan, R. C. Bansal, and V. K. Ramachandaramurthy, “A review of key power system stability challenges for large-scale PV integration,” Renewable & Sustainable Energy Reviews, vol. 41, pp. 1423–1436, Jan. 2015, doi: 10.1016/j.rser.2014.09.027.

[3] R. Rajan, F. M. Fernandez, and Y. Yang, “Primary frequency control techniques for large-scale PV-integrated power systems: A review,” Renewable & Sustainable Energy Reviews, vol. 144, p. 110998, Jul. 2021, doi: 10.1016/j.rser.2021.110998.

[4] T. Liu, Y. Song, L. Zhu, and D. J. Hill, “Stability and control of power grids,” Annual Review of Control, Robotics, and Autonomous Systems, vol. 5, no. 1, pp. 689–716, May 2022, doi: 10.1146/annurev-control-042820-011148.

[5] E. Proedrou, “A comprehensive review of residential electricity load profile models,” IEEE Access, vol. 9, pp. 12114–12133, Jan. 2021, doi: 10.1109/access.2021.3050074.

[6] A. Beláň et al., “Measurement of static frequency characteristics of home appliances in smart grid systems,” Energies, vol. 14, no. 6, p. 1739, Mar. 2021, doi: 10.3390/en14061739.

[7] S. Debbarma and A. Dutta, “Utilizing electric vehicles for LFC in restructured power systems using fractional order controller,” IEEE Transactions on Smart Grid, vol. 8, no. 6, pp. 2554–2564, Nov. 2017, doi: 10.1109/tsg.2016.2527821.

[8] H. Shabbir, M. U. Rehman, S. A. Rehman, S. K. Sheikh, and N. Zaffar, “Assessment of harmonic pollution by LED lamps in power systems,” 2014 Clemson University Power Systems Conference, Mar. 2014, doi: 10.1109/psc.2014.6808099.

[9] S. Lupi, M. Forzan, and A. Aliferov, Induction and direct resistance heating. 2015. doi: 10.1007/978-3-319-03479-9.

[10] A. Abbas and B. Chowdhury, "A Data-Driven approach for providing frequency regulation with aggregated residential HVAC units," 2019 North American Power Symposium (NAPS), Wichita, KS, USA, 2019, Pp. 1-6, Oct. 2019, doi: 10.1109/naps46351.2019.9000343.

[11] J. Milanovic et al., Modelling and aggregation of loads in flexible power networks. 2014, pp. 62–69. [Online]. Available: https://cris.unibo.it/handle/11585/305154

[12] M. Bennett and Y. Liu, "The impact of large-scale dynamic load modeling on frequency response in the U.S. Eastern Interconnection," International Journal of Electrical Power & Energy Systems, vol. 120, p. 105983, Sep. 2020, doi: 10.1016/j.ijepes.2020.105983.

[13] I. D. Pasiopoulou, E. O. Kontis, T. . Papadopoulos, and G. K. Papagiannis, "Effect of load modeling on power system stability studies," Electric Power Systems Research, vol. 207, p. 107846, Jun. 2022, doi: 10.1016/j.epsr.2022.107846.

[14] P. Cicilio and E. Cotilla-Sanchez, "Evaluating Measurement-Based dynamic load modeling techniques and metrics," IEEE Transactions on Power Systems, vol. 35, no. 3, pp. 1805–1811, May 2020, doi: 10.1109/tpwrs.2019.2949722.

[15] H. W. Qazi and D. Flynn, "Synergetic frequency response from multiple flexible loads," Electric Power Systems Research, vol. 145, pp. 185–196, Apr. 2017, doi: 10.1016/j.epsr.2017.01.007.

[16] Nuccio, Salvatore et al. "IEEE Std 1459–2010. IEEE Standard Definitions for the Measurement of Electric Power Quantities under Sinusoidal, Nonsinusoidal, Balanced or Unbalanced Conditions." , IEEE, 2010.

[17] Y. Shang, F. Sun, Q. Fang, B. Chen, and J. Xie, "A novel fault diagnosis strategy for LED lamps via light output time-frequency characteristics analysis and machine learning," Heliyon, vol. 9, no. 9, p. e19737, Sep. 2023, doi: 10.1016/j.heliyon.2023.e19737.

[18] A. J. Collin, "Advanced load modelling for power system studies," 2013. [Online]. Available: http://ethos.bl.uk/OrderDetails.do?uin=uk.bl.ethos.615353

[19] "Targeting 100% LED lighting sales by 2025 – Analysis - IEA," IEA, Sep. 01, 2022. https://www.iea.org/reports/targeting-100-led-lighting-sales-by-2025

[20] W. Chen, S. N. Li, and S. Y. R. Hui, "A comparative study on the circuit topologies for offline passive light-emitting diode (LED) drivers with long lifetime & high efficiency," IEEE, Sep. 2010, doi: 10.1109/ecce.2010.5617934.

[21] Statista, “Lamps & Lighting - Worldwide | Statista Market Forecast,” Statista. https://www.statista.com/outlook/cmo/furniture/lamps-lighting/worldwiderevenue

[22] A. Arif, Z. Wang, J. Wang, B. Mather, H. Bashualdo, and D. Zhao, “Load Modeling—A review,” IEEE Transactions on Smart Grid, vol. 9, no. 6, pp. 5986–5999, Nov. 2018, doi: 10.1109/tsg.2017.2700436.

[23] “Energimyndigheten Database,” The Swedish Energy Agency, 2022. https://pxexternal.energimyndigheten.se/pxweb/en/ (accessed Mar. 10, 2024).

[24] Y. A. Mobarak, A. M. Hemeida, A. El-Bahnasawy, M. M. Hamada, and N. Kannan, “Voltage and Frequency based Load Dependent Analysis Model for Egyptian Power System Network,” Journal of Advanced Research in Dynamic and Control Systems, vol. 11, pp. 971–978, Jan. 2019, [Online]. Available: https://www.jardcs.org/abstract.php?id=1390

[25] “NEMA Standards for Electrical Motors,” NEMA, NEMA MG1-12.42.

A

Appendix 1

The given MATLAB code is created to calculate the active and reactive power according to IEEE standards mentioned in this research. It is helpful for those cases when there are several sets of data structures.

```
clear all
clear all
%% Frequencies of interest
frequencies = 47:53;
sampling_time = 0.2e-3;  % 0.02 ms in seconds
num_samples = 10000;       % Number of samples

% Initialize a cell array to hold the power data and an array
for RMS values
powerData = cell(length(frequencies), 1);
qpowerData = cell(length(frequencies), 1);
rmsValues = zeros(length(frequencies), 1);
qrmsValues = zeros(length(frequencies), 1);
voltData = cell(length(frequencies), 1);
curData = cell(length(frequencies), 1);
rmsVolt = zeros(length(frequencies), 1);
rmsCur = zeros(length(frequencies), 1);
timeData= cell(length(frequencies), 1);

fs = 1 / sampling_time; % Hz, sampling frequency

% Loop through each frequency, load the corresponding file,
and extract power data
for idx = 1:length(frequencies)

    fn = frequencies(idx); % Hz, current frequency
    Tn = 1 / fn; % s, rated period
    wn = 2 * pi * fn; % rad/s, rated angular frequency
    Ns = round(fs / fn); % number of samples per electrical
          ...period

    % Generate the filename dynamically
```

```
filename = sprintf('L5p5W_%dHz.mat', frequencies(idx));
% Load the data from the MATLAB file
data = load(filename);
% Extract the power values (assuming the structure is
                    ...always named the same)
structName = fieldnames(data);
V = data.(structName{1}).Y(2).Data; % Extract voltage (Vpu)
I = data.(structName{1}).Y(1).Data; % Extract current (Ipu)

integral_vt = cumtrapz(V) * sampling_time; % Cumulative
                    ...trapezoidal integration

P = V .* I;

% Calculate RMS values
I_rms = rms(I);
V_rms = rms(V);
pf = cos(pi / 6); % Assuming a constant power factor,
                    ...replace if needed

% Active power calculation
P_cal = I_rms * V_rms * pf;

% Active power over time
len = length(V);
Pe = zeros(len, 1);
Qe = zeros(len, 1);

for k = 1:(len - Ns + 1)
    Pe(Ns + k - 1) = 1 / Tn * sum(P(k:Ns + k - 1) *
                    ...sampling_time);
    Qe(Ns + k - 1) = (wn / Tn) * sum(I(k:Ns + k - 1) .*
            ...integral_vt(k:Ns + k - 1) * sampling_time);
end
Pe(1:Ns - 1) = Pe(Ns);
Qe(1:Ns - 1) = Qe(Ns);

% Adjust the time vector to match the length of Pe and Qe
% Create a time vector that matches the length of Pe
time_truncated = (0:length(Pe) - 1) * sampling_time;

% Store the truncated time vector for each frequency
timeData{idx} = time_truncated;

curData{idx} = I;
powerData{idx} = Pe ;
```

```
    qpowerData{idx} = Qe;
    voltData{idx} = V;

    % Calculate the RMS values
    rmsValues(idx) = sqrt(mean(Pe.^2));
    qrmsValues(idx) = sqrt(mean(Qe.^2));
    rmsVolt(idx) = sqrt(mean(V.^2));
    rmsCur(idx) = sqrt(mean(I.^2));
end

% Find limits for y-axes
y_min = min(cellfun(@min, powerData));
y_max = max(cellfun(@max, powerData));
y_limits = [y_min - 1, y_max + 1];

yq_min = min(cellfun(@min, qpowerData));
yq_max = max(cellfun(@max, qpowerData));
yq_limits = [yq_min - 1, yq_max + 1];

y_min_Vpu = min(cellfun(@min, voltData));
y_max_Vpu = max(cellfun(@max, voltData));
y_limits_Vpu = [y_min_Vpu, y_max_Vpu  ];

%% Plotting the RMS values
figure(1);
plot(frequencies, rmsValues, 'LineWidth', 1.5);
set(gca, 'FontSize', 14);  % Set font size of the
                  ...current axes to 14
xlabel('Frequency (Hz)', 'FontSize', 18 );
                  ...% Make the x-axis label font size 18
ylabel('Active Power RMS (W)', 'FontSize', 18);
                   ...% Make the y-axis label font size 18
title('Active Power RMS for 5p5W Lamp Set at Each Frequency');
grid on

figure(2);
plot(frequencies, qrmsValues, 'LineWidth', 1.5);
set(gca, 'FontSize', 14);  % Set font size of the
                  ...current axes to 14
xlabel('Frequency (Hz)', 'FontSize', 18 );
                    ...% Make the x-axis label font size 18
ylabel('Reactive Power RMS (VAR)', 'FontSize', 18);
                    ...% Make the y-axis label font size 18
title('Reactive Power RMS for 5p5W Lamp Set at Each Frequency');
grid on
```

```
%% Plotting Power and Voltage over Time
colors = lines(length(frequencies));
            ...% Get a set of distinct colors

% Split the frequencies into two groups for better
                              ...subplot arrangement
split_idx = ceil(length(frequencies) / 2);
freq_groups = {frequencies(1:split_idx),
                              ...frequencies(split_idx+1:end)};
P_groups = {powerData(1:split_idx), powerData(split_idx+1:end)};
Q_groups = {qpowerData(1:split_idx), qpowerData(split_idx+1:end)};
V_groups = {voltData(1:split_idx), voltData(split_idx+1:end)};
V_rms_groups = {rmsVolt(1:split_idx), rmsVolt(split_idx+1:end)};
% Plot active power and voltage for the first group
figure;
for idx = 1:length(freq_groups{1})
    subplot(length(freq_groups{1}), 1, idx);

    % Plot active power on the left y-axis
    yyaxis left
    plot(timeData{idx}, P_groups{1}{idx}, 'Color',
            ...colors(idx, :), 'LineWidth', 1.5);
    set(gca, 'FontSize', 14); % Set font size of the
                              ...current axes to 14
    xlabel('Time (seconds)', 'FontSize', 18 );
                         ...% Make the x-axis label font size 18
    ylabel('Active Power (W)', 'FontSize', 18, 'Color',
        ...colors(idx, :)); % Make the y-axis label font size 18
    ylim(y_limits);
    xlim([0 2]);

    % Plot voltage on the right y-axis
    yyaxis right
    yline(V_rms_groups{1}(idx), 'Color', 'r', 'LineWidth', 1.5);
    set(gca, 'FontSize', 14); % Set font size of the
                              ...current axes to 14
    xlabel('Time (seconds)', 'FontSize', 18);
                           ...% Make the x-axis label font size 18
    ylabel('Voltage (V)', 'FontSize', 18,'Color','r');
                            ...% Make the y-axis label font size 18
    ylim(y_limits_Vpu);
    xlim([0 2]);

    title(sprintf('Voltage and Active Power over Time for
                ...5p5W Lamp Set at %d Hz', freq_groups{1}(idx)));
    xlabel('Time (seconds)');
```

```
    grid on;
end

% Plot active power and voltage for the second group
figure;
for idx = 1:length(freq_groups{2})
    subplot(length(freq_groups{2}), 1, idx);

    % Plot active power on the left y-axis
    yyaxis left
    plot(timeData{idx+split_idx}, P_groups{2}{idx}, 'Color',
            ...colors(idx+4, :), 'LineWidth', 1.5);
    set(gca, 'FontSize', 14);  % Set font size of the
                                ...current axes to 14
    xlabel('Time (seconds)', 'FontSize', 18 );
                              ...% Make the x-axis label font size 18
    ylabel('Active Power (W)', 'FontSize', 18, 'Color',
        ...colors(idx+4, :));  % Make the y-axis label font size 18
    ylim(y_limits);
    xlim([0 2]);

    % Plot voltage on the right y-axis
    yyaxis right
    yline(V_rms_groups{1}(idx), 'Color', 'r', 'LineWidth', 1.5);
    set(gca, 'FontSize', 14);  % Set font size of the
                          ...current axes to 14
    xlabel('Time (seconds)', 'FontSize', 18);
                          ...% Make the x-axis label font size 18
    ylabel('Voltage (V)', 'FontSize', 18,'Color','r');
                         ...% Make the y-axis label font size 18
    ylim(y_limits_Vpu);
    xlim([0 2]);

    title(sprintf('Voltage and Active Power over Time for
               ...5p5W Lamp Set at %d Hz', freq_groups{2}(idx)));
    xlabel('Time (seconds)');
    grid on;
end

%% Plot reactive power and voltage over time
% Plot reactive power and voltage for the first group
figure;
for idx = 1:length(freq_groups{1})
    subplot(length(freq_groups{1}), 1, idx);

    % Plot reactive power on the left y-axis
```

```
    yyaxis left
    plot(timeData{idx}, Q_groups{1}{idx}, 'Color',
                              ...colors(idx, :), 'LineWidth', 1.5);
   set(gca, 'FontSize', 14);  % Set font size of the
                                ...current axes to 14
    xlabel('Time (seconds)', 'FontSize', 18);
                              ...% Make the x-axis label font size 18
    ylabel('Reactive Power (VAR)', 'FontSize', 18, 'Color',
         ...colors(idx, :));  % Make the y-axis label font size 18
    ylim(yq_limits);
     xlim([0 2]);

    % Plot voltage on the right y-axis
    yyaxis right
    yline(V_rms_groups{1}(idx), 'Color', 'r', 'LineWidth', 1.5);
    set(gca, 'FontSize', 14);  % Set font size of the
                                    ...current axes to 14
    xlabel('Time (seconds)', 'FontSize', 18);
                              ...% Make the x-axis label font size 18
    ylabel('Voltage (V)', 'FontSize', 18,'Color','r');
                            ...% Make the y-axis label font size 18
    ylim(y_limits_Vpu);
     xlim([0 2]);

    title(sprintf('Voltage and Reactive Power over Time for
               ...5p5W Lamp Set at %d Hz', freq_groups{1}(idx)));
    xlabel('Time (seconds)');
    grid on;
end

% Plot reactive power and voltage for the second group
figure;
for idx = 1:length(freq_groups{2})
    subplot(length(freq_groups{2}), 1, idx);

    % Plot reactive power on the left y-axis
    yyaxis left
    plot(timeData{idx+split_idx}, Q_groups{2}{idx}, 'Color',
            ...colors(idx+split_idx, :), 'LineWidth', 1.5);
    set(gca, 'FontSize', 14);  % Set font size of the
                               ...current axes to 14
    xlabel('Time (seconds)', 'FontSize', 18);
                       ...% Make the x-axis label font size 18
    ylabel('Reactive Power (VAR)', 'FontSize', 18, 'Color',
      ...colors(idx+split_idx, :));
                   ....% Make the y-axis label font size 18
```

```
    ylim(yq_limits);
     xlim([0 2]);

    % Plot voltage on the right y-axis
    yyaxis right
    yline(V_rms_groups{1}(idx), 'Color', 'r', 'LineWidth', 1.5);
    set(gca, 'FontSize', 14);  % Set font size of the
                                         ...current axes to 14
    xlabel('Time (seconds)', 'FontSize', 18);
                                ...% Make the x-axis label font size 18
    ylabel('Voltage (V)', 'FontSize', 18,'Color','r');
                                ...% Make the y-axis label font size 18
    ylim(y_limits_Vpu);
     xlim([0 2]);

    title(sprintf('Voltage and Reactive Power over Time for
                 ...5p5W Lamp Set at %d Hz', freq_groups{2}(idx)));
    xlabel('Time (seconds)');
    grid on;
end

%% Percentage Deviation of Power at 50 Hz
% Find the RMS active and reactive power at 50 Hz
idx_50Hz = find(frequencies == 50);
Pe_50Hz = rmsValues(idx_50Hz);
Qe_50Hz = qrmsValues(idx_50Hz);

% Calculate percentage deviation for active and reactive power
Pe_deviation = (rmsValues - Pe_50Hz) / Pe_50Hz * 100;
Qe_deviation = (qrmsValues - Qe_50Hz) / Qe_50Hz * 100;

% Plotting the deviations
figure;

subplot(2, 1, 1);
bar(frequencies, Pe_deviation, 'FaceColor', [0.3010 0.7450 0.9330]);
set(gca, 'FontSize', 14);  % Set font size of the
                                ...current axes to 14
ylabel('Active Power (W)', 'FontSize', 18);
                         ...% Make the y-axis label font size 18
title('Percentage Deviation of Active Power from 50 Hz');
grid on;
ylim([-max(abs(Pe_deviation)) - 1, max(abs(Pe_deviation)) + 1]);

% Annotate the bar chart
for idx = 1:length(frequencies)
```

```
    if frequencies(idx) ~= 50
        text(frequencies(idx), Pe_deviation(idx),
        ... sprintf('%.2f%%', Pe_deviation(idx)), ...
            'VerticalAlignment', 'cap', 'HorizontalAlignment',
            ...'center','FontSize', 12, 'FontWeight',
            ...'bold', 'Color', 'k');
    end
end

subplot(2, 1, 2);
bar(frequencies, Qe_deviation, 'FaceColor', [0.9290 0.6940 0.1250]);
set(gca, 'FontSize', 14);  % Set font size of the
                           ...current axes to 14
ylabel('Active Power (W)', 'FontSize', 18);
                          ...% Make the y-axis label font size 18
title('Percentage Deviation of Reactive Power from 50 Hz');
grid on;
ylim([-max(abs(Qe_deviation)) - 1, max(abs(Qe_deviation)) + 1]);

for idx = 1:length(frequencies)
    if frequencies(idx) ~= 50
        text(frequencies(idx), Qe_deviation(idx),
                ...sprintf('%.2f%%', Qe_deviation(idx)), ...
            'VerticalAlignment', 'bottom', 'HorizontalAlignment',
            'center', 'FontSize', 12, 'FontWeight',
            ...'bold', 'Color', 'k');
    end
end
```

DEPARTMENT OF SOME SUBJECT OR TECHNOLOGY
CHALMERS UNIVERSITY OF TECHNOLOGY
Gothenburg, Sweden
www.chalmers.se

CHALMERS
UNIVERSITY OF TECHNOLOGY